Atmos. Chem. Phys., 25, 263–289, 2025
https://doi.org/10.5194/acp-25-263-2025

Atmospheric Chemistry and Physics
Open Access
EGU

Research article

Maximum ozone concentrations in the southwestern US and Texas: implications of the growing predominance of the background contribution

David D. Parrish[1], **Ian C. Faloona**[2,3], **and Richard G. Derwent**[4]

[1]David.D.Parrish, LLC, 4630 MacArthur Ln, Boulder, Colorado, USA
[2]Air Quality Research Center, University of California, Davis, Davis, CA, USA
[3]Department of Land, Air, and Water Resources, University of California, Davis, Davis, CA, USA
[4]rdscientific, Newbury, Berkshire, UK

Correspondence: David D. Parrish (david.d.parrish.llc@gmail.com)

Received: 5 February 2024 – Discussion started: 4 March 2024
Revised: 26 October 2024 – Accepted: 30 October 2024 – Published: 9 January 2025

Abstract. We utilize a simple, observation-based model to quantitatively estimate the US anthropogenic, background and wildfire contributions to the temporal and spatial distributions of maximum ozone concentrations throughout the southwestern US, including Texas and parts of California. The very different temporal variations in the separate contributions provide the basis for this analysis: over the past 4 decades the anthropogenic contribution has decreased at an approximately exponential rate by a factor of ∼6.3, while the US background concentration rose significantly through the 1980s and 1990s, reached a maximum in the mid-2000s, and has since slowly decreased. We primarily analyze ozone design values (ODVs), the statistic upon which the US National Ambient Air Quality Standards (NAAQS) are based. The ODV is an extreme value statistic that quantifies the relatively rare maximum observed ozone concentrations; thus, ODV time series provide spatially and temporally resolved records of maximum ozone concentrations throughout the country. Recent contributions of US background ozone to ODVs (primarily due to transported baseline ozone) are 64–70 ppb (parts per billion) over most of the southwestern US, and wildfires (also generally considered a background contribution) add further enhancements of 2–6 ppb in southwestern US urban areas. US anthropogenic emissions from urban and industrial sectors now produce only relatively modest enhancements to ODVs (less than ∼6 ppb in 2020) outside of the three largest urban areas considered (Dallas, Houston and Los Angeles), where the 2020 enhancements were in the 17–30 ppb range. As a consequence, US background ozone concentrations now dominate over US anthropogenic contributions in the western US, including the Los Angeles urban basin, where the largest US ozone concentrations are observed. In the southwestern US, this predominance is so pronounced that the US background plus wildfire contributions to ODVs approach or exceed the US NAAQS threshold for ozone of 70 ppb (implemented in 2015) and 75 ppb (implemented in 2008); consequently, NAAQS achievement has been precluded in this region. The large background contribution in this region has led to a pronounced shift in the spatial distribution of maximum US ozone concentrations; once ubiquitous nearly nationwide, ODVs of 75 ppb or greater have nearly disappeared in the eastern US, but such values are still frequent in the southwestern US. By 2021, the trend in maximum ODVs in two of the more highly populated eastern urban areas (i.e., New York City and Atlanta) had decreased to the point that they were smaller than those in significantly less populated southwestern US urban areas and nearly as small as ODVs recorded at isolated rural southwestern US sites. Two implications arise from these findings. First, alternate emission control strategies may provide more effective approaches to ozone air quality improvement; as background ozone makes the dominant contribution to even the highest observed concentrations, an international effort to reduce northern midlatitude baseline ozone concentrations could be pursued, or a standard based on the anthropogenic increment above the regionally varying US

background ozone concentration could be considered to provide a regionally uniform emission reduction challenge. Second, the predominant contribution of US background ozone across the southwestern US presents a profound challenge for air quality modeling, as a manifold of stratospheric and tropospheric processes occurring at small spatial scales but over hemisphere-wide distances must be accurately treated in detail to predict present and future background contributions to daily maximum ozone concentrations at local scales.

1 Introduction and background

Elevated ambient ozone (O_3) concentrations constitute an air quality issue that has affected many urban areas of the world; in Los Angeles, they reached extreme levels, with maximum 1 h average ozone concentrations exceeding 500 ppb (parts per billion) in the mid-1960s (Parrish and Stockwell, 2015). In the US, large reductions in anthropogenic emissions of photochemical ozone precursors, following the implementation of air quality improvement policies, substantially lowered urban ozone concentrations throughout the country over the past half-century. However, several areas have still not attained the National Ambient Air Quality Standards (NAAQS) threshold value for ozone (see https://www.epa.gov/green-book, last access: 3 February 2024). The NAAQS, most recently lowered in 2015, require that the ozone design value (ODV) at each monitoring site in a region not exceed 70 ppb (where ppb is equal to nanomoles of O_3 per mole of air). Notably, the 2008 NAAQS requirement is still in effect; even though this standard allows a higher ODV (75 ppb), there are different sets of nonattainment areas designated under the two standards. The ODV is an extreme value statistic defined as the 3-year average of the annual fourth-highest daily maximum 8 h average (MDA8) ozone concentration. The fourth-highest MDA8 represents the ∼98th percentile of MDA8 values observed in the warm half of the year, when those four highest values generally occur; thus, a time series of ODVs observed at a particular monitoring site is a smoothed record of the temporal evolution of the maximum ozone concentrations impacting that location. Ozone monitoring within the US began in the early 1970s, so ODVs have been collected over nearly 5 decades at more than 2000 sites throughout the nation. This observational record reflects detailed, spatially and temporally resolved information regarding the variability in ozone sources and sinks that determine the maximum observed ozone concentrations. Our goal in this paper is (1) to analyze this record to quantify the sources of maximum ozone concentrations in the southwestern US and (2) to investigate the implications of the results. This region has not previously been analyzed using our approach, but it is of particular interest because it is impacted by large background ozone concentrations (e.g., Lin et al., 2012a, b; Zhang et al., 2020). Previous work has shown that the background contributions to ODVs in some western US regions exceed 60 ppb (e.g., Langford et al., 2022) and have even approached 70 ppb, making achievement of the 70 ppb NAAQS threshold quite difficult in those regions (Cooper et al., 2015). The five states – Arizona (AZ), Colorado (CO), Nevada (NV), New Mexico (NM) and Utah (UT) – included in this region have four urban areas – Phoenix AZ, Denver CO, Las Vegas NV and Salt Lake City UT – that are centers of Marginal or Moderate ozone nonattainment areas (see *US EPA Green Book 8-Hour Ozone (2015) Area Information*, https://www.epa.gov/green-book/green-book-8-hour-ozone-2015-area-information, last access: 27 January 2023); additionally, Phoenix AZ and Denver CO are classified as respective Moderate and Severe-15 ozone nonattainment areas under the 2008 ozone NAAQS (see *US EPA Green Book 8-Hour Ozone (2008) Area Information*, https://www.epa.gov/green-book/green-book-8-hour-ozone-2008-area-information, last access: 27 January 2023). We also include Texas in this analysis because it represents a transition region between the southwestern US and the very different Gulf of Mexico region; four Texan urban areas – Dallas, Houston, El Paso and San Antonio – are centers of Marginal to Moderate ozone nonattainment areas designated under the 2015 NAAQS (*US EPA Green Book 8-Hour Ozone (2015) Area Information*, https://www.epa.gov/green-book/green-book-8-hour-ozone-2015-area-information); additionally Houston and Dallas are classified as Severe-15 nonattainment areas under the 2008 ozone NAAQS (*US EPA Green Book 8-Hour Ozone (2008) Area Information*, https://www.epa.gov/green-book/green-book-8-hour-ozone-2008-area-information). We examine the ODV time series recorded in these four urban areas as well as in five other regions in Texas containing smaller cities and vast rural areas.

Our analysis is a simple, observation-based quantification based on a conceptual model of the ozone sources that determine ODVs throughout the US. Notably, this approach is very different from the computer-based chemical transport models (CTMs) that have traditionally been used for such quantifications; this paper concludes with Sect. 5.5 that compares and contrasts these two approaches and discusses how they complement each other. Our analysis has previously been applied in the western US (Parrish et al., 2017, 2022) and the northeastern US (Parrish and Ennis, 2019). It focuses on the two major contributors to ODVs in both urban and rural areas. The first is the *US background ODV* (i.e., the ODV that would be recorded at a site in the absence of any contri-

bution from US anthropogenic emissions); this is the natural and anthropogenic ozone transported from outside the country plus any ozone produced within the US from naturally emitted precursors. This quantity provides a direct quantification of the minimum ODV that could be achieved by reducing US anthropogenic precursor emissions alone. The second is the *US anthropogenic ODV enhancement* (i.e., the enhancement of an actual ODV above the US background ODV due to contributions from US anthropogenic emissions); this enhancement is due to photochemical production from US anthropogenic emissions of ozone precursors. These definitions are consistent with the more general term *US background ozone* (USB), which is defined by the US Environmental Protection Agency (e.g., Dolwick et al., 2015) to represent the influence of all sources other than US anthropogenic emissions on a particular ozone concentration. Importantly, neither the US background ODV nor the USB can be directly measured, as they are theoretical constructs; the measured ozone concentration in air transported to a location without recent local or regional anthropogenic or continental influences is termed baseline ozone, and it may be closely related to USB (as will be discussed later). We separately quantify the US background ODV and the US anthropogenic ODV enhancement based on their very different long-term temporal changes. This quantification process fits time-dependent functions to tabulated ODV time series. As discussed below, these fitted functions have been designed to accurately represent the known temporal changes in the ODV components. The fitting process yields the values of parameters in those functions, and it is these values that quantify the ODV components. The text box (Box 1; which is very similar to that included in Parrish et al., 2022) collects the important terms discussed above (with their definitions) and the parameters included in the time-dependent functions discussed below.

Prevailing westerly winds carry midlatitude Pacific marine air into the western US, and the baseline ozone in that air provides the predominant source of the US background ODV in the aforementioned region (Zhang et al., 2020; Parrish et al., 2022). Parrish et al. (2020) show that the temporal change in baseline ozone at northern midlatitudes from 1978 to 2018 is accurately quantified by a quadratic polynomial, where t represents time:

$$\text{baseline } O_3 = a + bt + ct^2. \quad (1)$$

We use this same functional form to estimate the temporal variation in the US background ODVs. In this work, the time origin is chosen as the year 2000 (i.e., t equals the year $-$ 2000). Thus, the parameter a (in parts per billion of O_3) is the intercept of this function in 2000. The value of this parameter varies with location and quantifies the magnitude of the baseline ozone concentration in that year. The second and third coefficients in Eq. (1) quantify the variability in the baseline ozone before and after 2000. Parrish et al. (2020) derived numerical values for these parameters – $b = 0.20 \pm 0.06$ ppb yr^{-1} and $c = -0.018 \pm 0.006$ ppb yr^{-2} – that were common to eight northern midlatitude baseline ozone time series measured from surface sites, aircraft and sondes over western Europe and western North America covering altitudes from sea level to 9 km. These same coefficient values well represent 28 published trend analyses of baseline representative data sets collected throughout the western US (Parrish et al., 2021a). We use these same coefficient values in this work. The positive value of b and the negative value of c indicate that baseline ozone concentrations increased before 2000, reached a maximum after 2000 and then decreased at later times. Equation (2) gives the year of the maximum of the fitted curve,

$$\text{year}_{\max} = -b/2c + 2000, \quad (2)$$

which is $\sim$ 2006 for the above parameter values.

Parrish et al. (2017) show that the US anthropogenic ODV enhancement in US urban areas has decreased rapidly over the past 4 decades, a decrease accurately captured by an exponential term with an e-folding time of $\sim$ 22 years; this corresponds to a decrease of a factor of more than 6 from 1980 to 2020. This behavior contrasts markedly with the much smaller changes that occurred in baseline ozone concentrations. Parrish et al. (2017) and Parrish and Ennis (2019) assumed that baseline ozone remained constant, while Parrish et al. (2022) used Eq. (1) to quantify the changes that have occurred in the US background ODV near the US western coast. Equation (3) defines a simple functional form that captures the physical picture of a US background ODV that slowly varies, similarly to baseline ozone concentrations, plus a rapidly decreasing US anthropogenic ODV enhancement;

$$\begin{aligned} \text{ODV} &= a + bt + ct^2 + A\exp(-t/\tau) \\ &= a + 0.20 \times t - 0.018 \times t^2 + A \times \exp(-t/\tau), \end{aligned} \quad (3)$$

where the values of the b and c parameters derived by Parrish et al. (2020) have been substituted into the second form of the equation. Here, A is the year 2000 magnitude of the exponential term designed to quantify the rapidly decreasing US anthropogenic ODV enhancement, τ is the time constant of that exponential decrease and t equals the year $-$ 2000, as in Eq. (1). An exponential function is chosen to quantify the long-term decrease in US anthropogenic ODV enhancements, because it is mathematically as simple as possible (i.e., has the fewest possible unknown parameters) and successfully accounts for a large fraction of the variance in recorded ODV time series throughout the US (see Parrish et al., 2017, 2022; Parrish and Ennis, 2019); this choice is more fully discussed in Sects. S3 and S4 in the Supplement. Regression fits of Eq. (3) to ODV time series are the primary basis for analysis in this work; values are derived for the a and A parameters, which provide quantitative estimates of the year 2000 US background ODV and year 2000 US an-

- **MDA8** - Maximum daily 8-hour average ozone concentration at a site on a particular day.
- **Ozone Design Value (ODV)** - 3-year running mean of the annual fourth-highest MDA8 ozone concentration at a site.
- **Baseline ozone** - The ozone concentration measured in air transported to a location without recent local or regional anthropogenic or continental influences, typically derived from observations.
- **US background ozone (USB)** - The ozone concentration that would exist at a time and US location from all sources, except that produced from US anthropogenic emissions, typically derived by zeroing out emissions in chemical transport models.
- **US background ODV** – The ODV that would be recorded at a site in the absence of any contribution from US anthropogenic emissions.
- **US anthropogenic ozone ODV enhancement** – The enhancement of an actual ODV above the US background ODV due to contributions from US anthropogenic emissions.
- a – Fit parameter of Eqs. 1, 3 and 4 that estimates the US background ODV in year 2000.
- A – Fit parameter of Eq. 3 that estimates the US anthropogenic ODV in year 2000.
- τ – Fit parameter of Eq. 3 that estimates the exponential rate of decrease of the US anthropogenic ozone (or ODV) enhancement with time.

Box 1. Important quantitative terms and parameters with definitions.

thropogenic ODV enhancement, respectively. The definitions of the three parameters in Eq. (3) are included in Box 1.

Parrish et al. (2022) applied the above-described analysis to the entire western US coastal region; they quantify a small negative latitude gradient (−0.4 ppb per degree) and a strong positive vertical gradient ($\sim$ 10–15 ppb km^{-1}) in the US background ODVs at monitoring sites along the US western coast. The latitude gradient is consistent with earlier model and observational analysis (Zhang et al., 2020; Ziemke et al., 2011). The altitude gradient agrees well with that determined by sondes and aircraft profiles along the coast of California (Oltmans et al., 2008; Cooper et al., 2011; Yates et al., 2015; Faloona et al., 2020); however, this vertical gradient is weakened by continental mixing as marine air is advected eastward across the complex terrain of the North American Cordillera. The quantification of such fine-scale variations (on the order of 1–2 ppb) provides a sense of the analysis precision, and the agreement with other analyses is evidence that the results of the observation-based quantification are physically realistic. Nevertheless, it is important to draw a careful distinction between the definitions of US background ODV and US anthropogenic ODV enhancement presented above and their observation-based quantifications that we derive. As those quantifications rely on the observed temporal changes in ODVs, only sources of precursors effectively controlled by regulatory action can contribute to the derived A-parameter value, i.e., the estimated US anthropogenic ODV enhancement. The impact of uncontrolled anthropogenic precursor emissions (e.g., those from agricultural soils, livestock operations or volatile chemical products) would potentially contribute to the a-parameter value, i.e., the estimated US background ODV. Those drawing conclusions from the derived quantifications must carefully consider this issue and bring in additional considerations to avoid confounding influences. Temporal changes in emissions from wildfires are another potentially confounding influence; Sect. 3.2 discusses our approach to including these changes in our analysis. Furthermore, the ODVs represent rare events that may occur at any time during the warm season when the combined USB and anthropogenic ozone contributions reach their maximum. This maximum may not occur on the days when the USB contribution is largest (i.e., the days that determine the US background ODV). Thus, for any given extreme ozone episode, the sum of US background ODV and the anthropogenic contribution to that episode may not equal the observed ODV; Sect. S2 in the Supplement discusses the distinction between the US anthropogenic ODV enhancement and the actual anthropogenic contribution to an ODV in detail.

In this work, we extend the observation-based analysis of ODV time series to the southwestern US and Texas; we also survey surrounding states, including an analysis of the distributions of MDA8 ozone concentrations in Californian air basins. This quantification of the spatial and temporal variability in the US background ODV is important to improve our understanding of the magnitude and temporal changes in the primary ozone sources, to quantify how the growing dominance of USB has changed the regional distribution of occurrence of ozone air quality standard exceedances, and to discuss the implications for future efforts to improve US ozone air quality. In the following, Sect. 2 describes the data set that is the basis for this analysis, Sect. 3 discusses details of the analysis approach, Sect. 4 presents the results, and Sect. 5 discusses the conclusions and implications.

2 Data sets analyzed

This work examines two data sets: (1) MDA8 ozone concentrations measured during the 1980–2022 period in four coastal Californian air basins and (2) ODVs reported from the beginning of US ozone monitoring through 2021 throughout the US. The California MDA8 ozone concentrations were obtained from the California Air Resources Board data archive (https://www.arb.ca.gov/adam/index.html, last

access: 10 October 2023). The ODVs are computed and published annually by US EPA's Office of Air Quality Planning and Standards. For each year for each ozone monitoring station in the US, an ODV is calculated if the measurements achieve the specified completeness criteria. All values reported in the focus region were downloaded from the EPA data archive (https://www.epa.gov/aqs, last access: 9 November 2023); however, only the ODVs marked as valid were retained for analysis. Exceptional events, such as wildfires or stratospheric ozone intrusions, are included in the data set, although in principle they can be removed from the MDA8 monitoring record through an EPA concurrence process as uncontrollable "Exceptional Events", thereby altering the ODV archive; nevertheless, the analysis presented in this paper is not significantly affected because EPA has only rarely concurred in such removal in the present study region. Section S6 in the Supplement more fully discusses this issue.

Notably, very few sites report continuous MDA8 or ODV records over the entire monitoring period, with some sites operating for only a few years. Generally, we consider all reported values in our analysis, even if only a single ODV was reported from a particular site; any temporal discontinuity associated with initiation and termination of an individual site is assumed to still allow an accurate quantification of temporal trends within the selected region. Sensitivity tests have shown that analyses based on single sites with continuous records over the entire time period agree well with analyses of records combined from multiple sites with shorter-duration records within the same region.

The ozone data considered here include the time period of emission reductions resulting from societal efforts to control the COVID-19 pandemic. Many publications have examined the impacts of those emission reductions on ozone in areas throughout the world, with widely varying findings. No consistent impact has been found for summertime maximum ozone concentrations (e.g., Gkatzelis et al., 2021), which are the focus of this study. We find no apparent systematic deviations in MDA8 concentrations or ODVs reported for 2020 – the year of largest emission reductions – in any of the time series examined, so this issue is not considered further in this analysis.

3 Methods

3.1 Quantification of temporal changes in ODVs and MDA8 distribution percentiles

Our primary analysis relies on quantifying long-term changes in ODVs recorded during the entire ozone monitoring period in the southwestern US and surrounding states as well as in two contrasting states in the eastern US. As the ODVs are 3-year averages, their time series are insensitive to diurnal and seasonal variations, but they do reflect changes on decadal (systematic long-term changes) and subdecadal (i.e., interannual variability) timescales. Fits of simple, continuous functional forms to the time series provide objective quantification of the average long-term changes. The parameter values derived from fits of Eq. (3) are the basis for the discussion of regional similarities and differences in ODV time series. The analysis utilized here is the generally the same as that of Parrish et al. (2022), which is reviewed in Sect. 1, with the additional development of an estimate for the average long-term contribution of wildfire emissions to urban ODVs (Sect. 3.2). We also fit Eq. (1) to the ODVs recorded at some isolated rural sites in the western US (Sect. 4.1) to verify that the b- and c-parameter values quantified by Parrish et al. (2020) are appropriate for general application to southwestern US ODVs.

In addition, we analyze the distribution of MDA8 ozone concentrations recorded in four coastal Californian air basins; these concentrations vary between days and among seasons as well as on the longer timescales that affect the ODVs. As our focus is on maximum ozone concentrations, we only consider the largest MDA8 ozone concentration observed at any of the sites in a given air basin on each day during the ozone season, which we take as May through September. Note that the site recording the largest MDA8 in each basin can vary from day to day. This selection gives 153 MDA8 values in each year in each basin. From these 153 values, we characterize each year's distribution of these values by calculating seven percentiles of the distribution: minimum, 10th, 25th, median, 75th, 90th and maximum. The time series of each of these percentiles can then be fit to the same continuous functional form (i.e., Eq. 3) as fit to the ODV time series. The a- and A-parameter values derived in these fits then provide estimates of the year 2000 USB contribution and the US anthropogenic enhancement for the respective percentiles. Parrish et al. (2016) utilized a similar approach in their analysis of the largest MDA8 ozone concentrations recorded in the South Coast Air Basin (SoCAB), one of the coastal Californian air basins also considered in this work.

Quantified uncertainties in the parameter values derived from the functional fits are important in our analysis; the 95 % confidence limits are utilized, unless indicated otherwise. These confidence limits are derived from the fitting procedures utilized in the analysis. The confidence limits from the ODV fits are widened to account for the known covariance between the recorded ODVs. Each ODV is a 3-year running mean, so only every third ODV is independent from the others at a given site. Consequently, the number of independent ODVs in each fit is approximately a factor of 3 smaller than the number of reported ODVs, and the fitting routines therefore underestimate the true confidence limits of the derived parameters. All reported confidence limits are increased by a factor of $3^{1/2}$ to account for this covariance (Parrish et al., 2022). Additional sources of covariance (regionally coherent interannual variability, temporal interannual variability, etc.) may exist between values included in any particular fit; we cannot account for the influence of any such additional covariance.

An important issue in the present analysis is the derivation of the value of τ. The time series of urban ODVs investigated here do not allow for the simultaneous derivation of precise values for all three (a, A and τ) parameters of Eq. (3). This difficulty is surmounted by assuming that the value of $\tau = 21.8 \pm 0.8$ years derived in earlier work for southern California (Parrish et al., 2022) is also appropriate for all regions considered here. A justification for this assumption is that precursor emission control strategies, particularly for on-road vehicles, implemented throughout the US have been similar to those in California; it is on-road vehicle emissions that have dominated urban ozone production over the past several decades (Nopmongcol et al., 2017). Parrish and Ennis (2019) also made this assumption for the northeastern US and presented several consistency checks showing that this assumption is appropriate for that region, which is further removed from southern California than the southwestern US region considered here. Section S5 in the Supplement further discusses the justification for this assumption in the southwestern US and the uncertainty in the derived value of τ.

3.2 Long-term temporal changes in wildfire contributions

ODV contributions from wildfire emissions can affect the results of analysis based on Eq. (3). These emissions have not been systematically reduced; rather, wildfire emissions are increasing as the climate warms (e.g., Westerling et al., 2006; Westerling, 2016). Parrish et al. (2022) discuss three characteristics of the impact of wildfire emissions on ODV time series: first, wildfire emissions alone do not significantly elevate ODVs, but when they mix with local NO_x emissions, such as in central urban areas, their impact can be discerned (e.g., McKeen et al., 2002; Parrish et al., 2022; see Sect. 5.5 for further discussion); second, wildfire impacts have systematically increased over past decades; and, third, wildfires are highly sporadic, both temporally and spatially. Addition of another term to Eq. (3) can account for the systematic, temporally increasing influence of wildfire emissions. Burke et al. (2021) estimate that the wildfire burned area in the US has roughly quadrupled in an approximately linear fashion over the past 4 decades (their Fig. 1a). Similarly, Iglesias et al. (2022) estimate that the annual mean area burned in the western US has risen by 220 %–330 % across a 20-year span within the period from 1984 to 2018 (their Fig. 7a). We represent the decadal-scale average ODV contribution from wildfires by a similar increase; Eq. (4) is Eq. (3) with an added term that increases linearly by a factor of 4 from 1980 to 2020. Here, the parameter WF represents the location-specific ODV enhancement due to wildfires in the year 2000, whereas A_{WF} represents a revised A parameter in locations where enhancements of ODVs due to wildfire emissions are significant.

$$\begin{aligned}\mathrm{ODV} = {} & a + 0.20 \times t - 0.018 \times t^2 + A_{\mathrm{WF}} \times \exp(-t/\tau) \\ & + \mathrm{WF} \times (1 + 0.03 \times t) \end{aligned} \quad (4)$$

The linear increase in the wildfire contribution does not account for the sporadic character of wildfires; however, this functional form is appropriate for the 3-year averaging period inherent in ODV time series. There are available databases giving the spatial and temporal distributions of the area burned by wildfires with detail that varies from annual means for the entire country (e.g., https://www.nifc.gov/fire-information/statistics/wildfires, last access: 7 February 2024) to monthly means for individual states (e.g., the monthly area burned in California from 1972 to the present is available from the California Department of Forestry and Fire Protection). However, to incorporate such detailed information into our analysis would require knowledge of the spatial and temporal variability in wildfire impacts on maximum ozone concentrations at individual sampling sites, which is not available without detailed atmospheric transport modeling. Therefore, year-to-year variation in wildfire impacts undoubtedly contributes to the variability in ODVs about the functional fits to the ODV time series discussed in this work; thus, higher ODV variability in an area may be indicative of an important wildfire influence.

In principle, fitting Eq. (4) to an ODV time series would allow for the determination of values for three parameters (a, A_{WF} and WF, with τ already fixed); however, in practice, such fits generally do not allow the precise determination of all three parameters. Nevertheless, if a can be determined from a separate analysis, precise values can be determined for A_{WF} and WF from fits of Eq. (4). We follow this approach in the analysis of time series of maximum ODVs recorded in southwestern US urban areas, which are the only areas in the region with large enough local NO_x emissions to cause significant enhancements of ODVs due to wildfire emissions. Additional complications can arise from ozone contributions produced from agricultural emissions or from other anthropogenic emissions that have not been as effectively controlled (compared with other anthropogenic emissions). Parrish et al. (2017, 2022) discuss such ODV contributions in intense agricultural regions of California; using GEOS-Chem, Geddes et al. (2022) modeled significant NO_x emissions from agricultural soils throughout the southwest, although especially in Texas and California. Parrish and Ennis (2019) discuss possible ODV contributions from volatile chemical products; their emissions history is not well quantified, but emissions are likely increasing (McDonald et al., 2018). Other ODV contributions that have not been controlled include those from oil and gas extraction processes, which are important in some regions of the southwestern US and have increased overall during the past decades; urban areas where such impacts have been studied include Denver–Front Range of Colorado (e.g., McDuffie et al., 2016) and Dallas–Fort Worth (e.g., Ahmadi and John, 2015). Depending upon their specific temporal dependence, ODV contributions from these uncontrolled emission sources could contribute to the "wildfire" term in Eq. (4) if they have been increasing, but none are expected to be doubling in magnitude

every 20 years as the parameterized wildfire source is here. Section S4 in the Supplement further discusses some issues regarding uncontrolled anthropogenic ozone precursor emissions.

3.3 Additional analysis considerations

Networks of ozone monitoring sites have operated in all of the largest US urban areas; the ODVs from several of these networks are examined in detail. Where possible, the full time periods of the data records are included in the analyses. However, the analysis based on Eqs. (3) and (4) can only represent the time period over which ODVs consistently decreased. In some urban areas consistent decreases did not begin until after measurements began, or the early data do not appear to accurately represent the overall urban area; in this case, the ODVs selected for analysis begin in a later year. The most extreme example of the latter case is Las Vegas, where several newly established measurement sites began reporting ODVs in 2000; these values were significantly larger than those reported from any other sites in that urban area. Thus, the analysis of the Las Vegas data is limited to 2000–2021 to avoid a discontinuity in the time series of ODVs. In the following section, the figures that illustrate the analyses include all recorded ODVs, so selection of ODVs for analysis can be examined.

The ODV time series fit to Eqs. (3) and (4) are either from single sites or multiple sites that are in reasonably close spatial proximity and exhibit similar temporal changes. There is some subjectivity in this selection of time series, which is guided by maximizing the temporal length of the series, minimizing confidence limits of the derived parameters, and minimizing deviations between the ODVs and the fits.

In addition to the confidence limits for derived parameter values, the quality of the fits of Eqs. (3) and (4) are quantified by root-mean-square deviations (RMSDs) between the fits and the recorded data, which scatter both above and below the fits; these RMSDs are generally in the range of 3–5 ppb (e.g., Tables S1 and S3–S5). These deviations are attributed to quasi-chaotic, varying ODV contributions from factors such as wildfires, stratospheric intrusions and variable meteorological conditions. Our observation-based model does not account for this residual variance.

4 Results

In the following sections, we analyze ODV time series recorded throughout the southwestern US and Texas as well as in surrounding and more distant states; moreover, we examine the full distribution of the largest MDA8 ozone concentrations in four Californian coastal air basins. Section 4.1 investigates the appropriateness of applying the b and c coefficients derived by Parrish et al. (2020) to the analysis of ODV time series recorded in the southwestern US. Section 4.2 analyzes the temporal evolution of the distribution of the MDA8 ozone concentrations in the Californian air basins, and the following three sections present the analysis of ODV time series in the southwestern US (Sect. 4.3), Texan urban and rural areas (Sect. 4.4), and some other US states to provide context (Sect. 4.5).

4.1 Long-term ODV changes at isolated rural sites in the western US

Investigation of time series of ODVs at remote, rural sites provides an opportunity to quantify the long-term changes in ODVs in regions where the US anthropogenic ODV enhancements are small. In the limit of zero US anthropogenic ODV enhancement, Eq. (3) is reduced to Eq. (1). Here, we (1) fit Eq. (1) to ODVs from such sites to derive b- and c-parameter values specific to the western US ODVs and compare those values to the values cited above from Parrish et al. (2020) and (2) fit Eq. (3) to these same time series to determine the small US anthropogenic ODV enhancement at those sites. Figure 1 shows ODV time series recorded at eight such sites included in the Clean Air Status and Trends Network (CASTNET) of the US EPA (https://www.epa.gov/castnet, last access: 9 December 2022); the locations are shown in the inset map. They are chosen to span a wide latitude range (32–48.5° N) and to be as isolated as possible from anthropogenic emission sources. Seven sites are in a relatively narrow longitude band (109.4–114.2° W) located ∼750–1100 km east of the US western coast, whereas the other is nearer (∼220 km) to the coast (Lassen Volcanic National Park, NP, at 121.6° W). All are at similar elevations (2.0 ± 0.43 km) except Glacier NP at 0.96 km.

Data from most of these same CASTNET sites have been included in previous studies of long-term ozone changes at western US rural and remote sites. Lassen Volcanic NP was investigated by Jaffe et al. (2003), Jaffe and Ray (2007), Parrish et al. (2009, 2012, 2017, 2020), and Cooper et al. (2014), due to the site's location near the US western coast. Another four of the sites (Glacier NP; Yellowstone NP; Craters of the Moon National Monument, NM; and Canyonlands NP) were also considered by Jaffe and Ray (2007). Two of the remaining sites (Great Basin NP and Grand Canyon NP) were included by Cooper et al. (2020) in their analysis of surface ozone trends at globally distributed remote sites. Here, we also consider Chiricahua NM, a more southerly site in Arizona. To our knowledge, these data sets comprise all of the longest, high-quality, relatively isolated rural data sets available in the western continental US.

The CASTNET time series of ODVs are illustrated in Fig. 1a. The curves are regression fits of Eq. (1), which quantify the long-term changes in baseline ozone. Table S1 gives the derived parameter values, along with confidence limits and the root-mean-square deviations (RMSDs) of the ODVs from the fits. The derived a-parameter values show that the absolute ODV values exhibit a systematic spatial gradient; there is close agreement among the largest

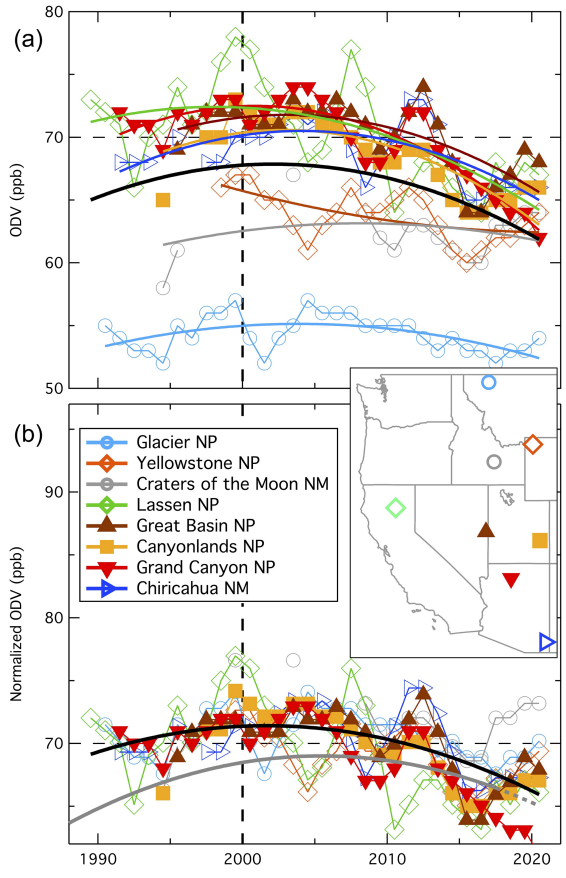

Figure 1. Time series of ODVs recorded at the eight rural western CASTNET sites shown in the inset map. Solid symbols indicate the three sites used for the normalization. Solid curves indicate the fits of Eq. (1) to **(a)** the individual site data (including the black curve fit to all data) and **(b)** all normalized data (black curve). The lower gray curve in panel **(b)** is the Parrish et al. (2020) fit to baseline data, normalized to 68.5 ppb (the a-parameter value derived in a fit of Eq. 3 to the normalized CASTNET data) in the year 2000; the dashed line shows an extrapolation of that fit to 2021.

a-parameter values at the five southern sites (weighted mean $= 71.5 \pm 0.8$ ppb and standard deviation $= 1.1$ ppb), with values decreasing with increasing latitude and/or decreasing elevation at the three more northern sites, reaching a minimum of 54.9 ± 1.1 ppb at Glacier NP, the most northern and lowest-elevation site. In contrast, the derived b and c coefficients at all sites agree within their confidence limits, which indicates the absence of a statistically significant difference in the temporal evolution of the ODVs among these widely separated sites, although substantial uncertainty remains in the determination of the coefficient values.

The similarity of the temporal evolution of these rural ODVs suggests normalizing the ODVs to remove the spatial gradient and to derive a single fit of Eq. (1) to all ODVs from the eight sites; the greater number of ODVs in a single fit then allows more precision in the determination of the derived parameter values. We choose to normalize to 71.4 ppb in the year 2000; this normalization factor is the average of the a parameters derived at Great Basin NP, Canyonlands NP and Grand Canyon NP (solid symbols in Fig. 1), which are chosen to represent the central southwestern US. The 212 normalized ODVs recorded over 32 years at the eight sites are fit within a RMSD of 2.4 ppb (Fig. 1b). This fit gives $b = 0.07 \pm 0.13$ ppb yr^{-1} and $c = -0.015 \pm 0.005$ ppb yr^{-2}; Table S1 indicates that all of the b and c parameters derived from the separate site fits agree with these values within their confidence limits. These parameter values indicate that the rural ODVs increased early in the data record, reached a maximum in year$_{max} = 2002 \pm 4$ and decreased thereafter. A linear fit to all of the normalized ODVs over the 2000–2021 period indicates a statistically significant average negative trend equal to -0.30 ± 0.10 ppb yr^{-1}.

The b- and c-parameter values derived here from the normalized CASTNET ODVs agree (within derived confidence limits; see Table 1) with the parameter values derived for the entire northern midlatitude region (Parrish et al., 2020). This agreement indicates that ODVs recorded at the eight CASTNET sites provide approximate, direct measures of southwestern US background ODVs and strongly support applying Eq. (3) for the analysis of ODV time series. (The derived d-parameter values in Table 1 indicate that a cubic term is not justified in the polynomial fit in either the analysis of Parrish et al. (2020) or the CASTNET ODVs.) The fit of Eq. (3), which includes the exponential term, to the normalized CASTNET ODVs is indistinguishable from the fit of Eq. (1) (black curve in Fig. 1b), although it does give a smaller value for the year 2000 US background ODV ($a = 68.5 \pm 1.5$ ppb, compared with 71.3 ± 0.8 for the fit to Eq. 1) with a small but significant anthropogenic ODV enhancement ($A = 2.8 \pm 1.9$ ppb). We interpret the final term of Eq. (3) as the mean ODV enhancement due to transport of ozone from US anthropogenic precursors to these isolated rural sites in the western US.

In summary, the second and third terms of Eq. (3) provide an accurate estimate of the long-term change in the mean US background ODV in the western US; these terms added to the derived a-parameter value of 68.5 ± 1.5 ppb, is plotted as the gray curve in Fig. 1b. Similar curves, normalized to a-parameter values derived in other fits, will be included in later graphs to illustrate the purely baseline contributions to ODV time series considered in the following analyses.

4.2 Contributions to MDA8 ozone concentration distributions in four coastal Californian air basins

Previous analyses have shown that Eq. (3) (or a closely related equation with a constant US background ODV term, rather than the small changes quantified by the second and third terms of Eq. 3) gives excellent fits to ODV time series (i.e., fits that capture a large fraction of the ODV variance and/or with relatively small RMSDs), not only in urban

Table 1. Parameter values (with 95 % confidence limits) derived from fits of Eq. (1) to time series baseline ozone concentrations. The d parameter represents the coefficient of the cubic term in the analogous fits to a third-order polynomial.

Data set	b (ppb yr^{-1})	c (10^{-2} ppb yr^{-2})	year$_{max}$	RMSD (ppb)	Reference	d (10^{-4} ppb yr^{-3})
The 2-year means of baseline ozone	0.20 ± 0.06	-1.8 ± 0.6	2005.7 ± 2.5	1.4	Parrish et al. (2020)	$+0.6 \pm 5.7$
The CASTNET ODVs – normalized*	0.07 ± 0.13	-1.5 ± 0.8	2002.1 ± 4.4	2.4	This work	$+5.8 \pm 10.1$

* The a-parameter value derived from the fit of Eq. (1) to the normalized CASTNET ODVs is 71.3 ± 0.8 ppb, which is consistent with the normalization process utilized here; the corresponding value in the Parrish et al. (2020) analysis was near zero due to the different normalization approach used in that work.

areas (Parrish et al., 2017, 2022; Parrish and Ennis, 2019) but also in relatively isolated northern rural states (Parrish et al., 2022) and at western US rural CASTNET (preceding section) and coastal (Parrish et al., 2022) sites. Here, we examine how well fit the entire distributions of the largest MDA8 ozone concentrations are in four coastal Californian air basins. These basins are selected to span a wide range of environments – the intensely photochemically active, highly urbanized South Coast Air Basin (SoCAB, containing the Los Angeles urban area) and San Diego AB, the highly urbanized but less photochemically active San Francisco Bay AB (SFB AB), and the rural North Coast AB – and to minimize impacts from uncontrolled anthropogenic emission sources, such as agricultural activity. Figure 2 illustrates the temporal evolution of seven percentiles of the MDA8 distributions; fits of Eq. (3) to the time series of each percentile are included, with the derived parameter values given in Table S2. The AB locations are indicated on the map inset in Fig. 3.

The fits of Eq. (3) are limited to the 36-year 1980–2015 period for most of the percentiles in the three urbanized air basins; later years are not included due to clear positive deviations of the higher percentiles of the distributions, most clearly in the SoCAB, whose cause or causes have not been established. One likely cause is the rise of a new regime of wildfire impacts. According to the California Department of Forestry and Fire Protection (CalFire) Fire and Resource Assessment Program (FRAP, https://www.fire.ca.gov/what-we-do/fire-resource-assessment-program, last access: 21 February 2024), 2007 was the first time in recorded history that California lost over 1×10^6 acres (4.05×10^3 km^2) in a year to wildfires; however, since then, the 4 highest wildfire years have occurred in 2020, 2021, 2018 and 2017, burning 4.1×10^6, 2.2×10^6, 1.8×10^6 and 1.3×10^6 acres (16.6×10^3, 8.9×10^3, 7.3×10^3, and 5.3×10^3 km^2), respectively. Although exact matches cannot be expected without detailed analysis of where each wildfire had its impacts, these years, particularly 2020, generally stand out in the recent maximum values evident in Fig. 2. In contrast, Kim et al. (2022) present a detailed investigation of these deviations in the SoCAB and conclude that they are caused by substantial recent changes in the photochemical regime in the aforementioned region. Note that the fits to the lowest percentile (i.e., the minimum MDA8) in the three urbanized air basins and to all percentiles in the rural North Coast Air Basin in Fig. 2 include the entire 43-year 1980–2022 period.

Despite the marked differences in the long-term changes between percentiles and basins evident in Fig. 2, the fits of Eq. (3) provide faithful descriptions of the long-term changes for all percentiles in all four basins; all RMSDs of the data about the fits are in the 2.5–9 ppb range (Table S2), except for the maxima, which exhibit larger variability. As expected, the anthropogenic enhancements (quantified by the derived A-parameter values) are largest in the SoCAB for all percentiles, except the minimum. The corresponding A-parameter values are approximately a factor of ~ 2 smaller in the San Diego AB than those in the SoCAB, and they are lower by another factor of ~ 2 in the SFB AB. In the North Coast AB region, all derived A-parameter values are near zero (-2.8 to 4.6 ppb); a significant negative A-parameter value indicates that the reaction of fresh NO_x emissions with USB has lowered observed MDA8 concentrations below those that would result from USB alone. Importantly, the fits to the North Coast AB percentiles are all qualitatively similar to the fits to the CASTNET ODVs in Fig. 1, exhibiting temporal behavior characteristic of baseline ozone; the fits to the minima in all four ABs also show qualitatively similar behavior with small A-parameter values ($< \sim 5$ ppb). This similarity indicates that transported baseline ozone concentrations dominate the lowest percentiles of observed MDA8 concentrations in all air basins, even in the SoCAB.

The derived a- and A-parameter values from the fits in Fig. 2 define the distributions of USB concentrations and US anthropogenic enhancements in the year 2000; Fig. 3a and b show bar graphs illustrating those distributions. By 2015, the distributions of these two ozone contributions had evolved as described by Eq. (3) to those shown in Fig. 3c and d. The US anthropogenic enhancements had decreased by a factor of 2.0 ($= \exp\{15/21.8\}$, based on the exponential term in Eq. 3), while the USB had decreased by only 1 ppb (difference in the first three terms of Eq. 3 between 2000 and 2015). Figure 3e illustrates the mean USB distribution, i.e., the average of the five separate USB distribution estimates in Fig. 3c, which is discussed further in Sect. 5.1.

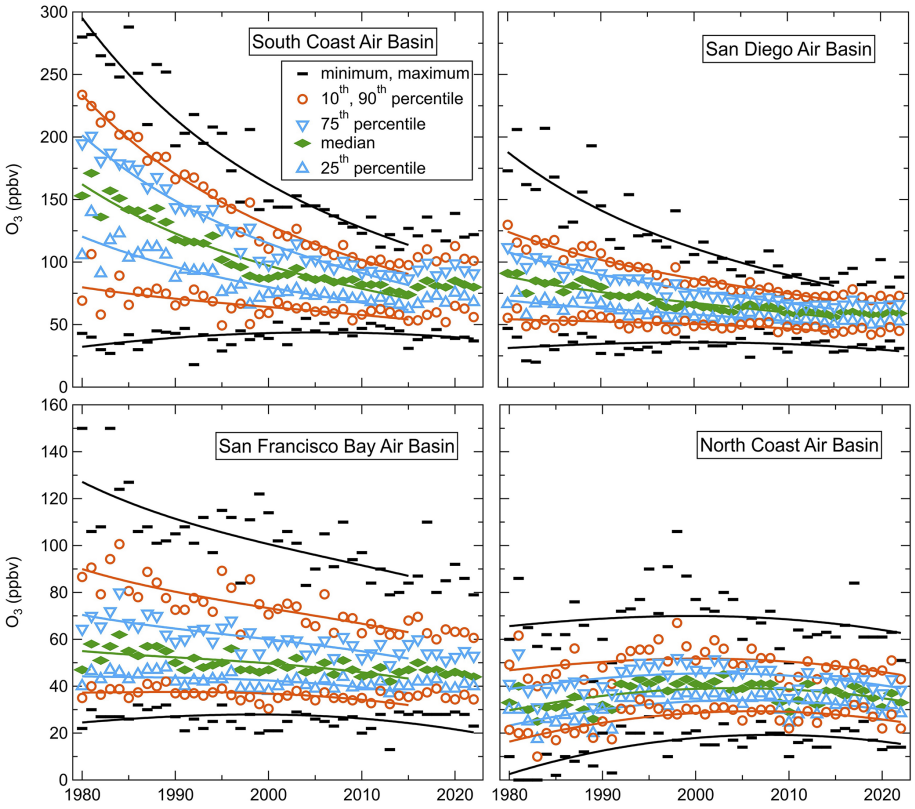

Figure 2. Temporal evolution of the distribution of MDA8 ozone concentrations in four Californian air basins. Symbols indicate the annotated percentiles of the annual distribution of the largest MDA8 concentration recorded at any monitor within the basin on each day of the May–September ozone season. Solid curves indicate fits of Eq. (3) to the respective percentiles.

4.3 ODV contributions in the southwestern US

The map in Fig. 4 shows the ozone monitoring site locations in seven southwestern US urban areas: four larger (Phoenix AZ, Denver CO, Las Vegas NV and Salt Lake City UT) and three smaller (Tucson AZ, Reno NV and the Albuquerque/Santa Fe NM area). Monitoring sites also sparsely cover the rural areas in these five states: 19 in Colorado, 9 in New Mexico, 6 in Utah, 8 in Arizona and 2 in Nevada, as shown on the map in Fig. S1. We examine the ODVs recorded at all of these urban and rural sites.

Figure 5 displays the analysis of the Denver CO urban (panel a) and Colorado rural (panel b) ODV time series. The urban ODVs generally fall above the fit to baseline data (black curve with dashed extension, which is reproduced from the gray curve in Fig. 1). One exception is the Camp site, with some ODVs falling well below the baseline curve; as this site is located at street level in central urban Denver, we attribute these small ODVs to reductions in observed ozone concentrations due to its reaction with fresh NO_x emissions. The rural data generally scatter about the baseline curve. Two rural sites that have received attention in previous work are emphasized as solid symbols. Gothic CO in western central Colorado (location indicated in Fig. S1) has been considered to be a remote site (Cooper et al., 2020); that ODV time series agrees with the baseline curve within an RMSD of 1.8 ppb. Rocky Mountain NP (location also indicated in Fig. S1) has been considered to be a high-elevation baseline site (Lin et al., 2017). The dashed green curves show fits of Eq. (3) to all ODVs in the urban (excluding the Camp site) and rural (excluding the Rocky Mountain NP site) data sets. The red curve shows the fit of Eq. (4), which includes possible wildfire influences, to the maximum urban ODVs. The parameter values from these fits are annotated in the figure and given to greater precision in Tables S3 and S4.

The derived a-parameter values from the analysis of Denver urban (69.0 ± 2.1 ppb) and Colorado rural (69.0 ± 3.1 ppb) ODVs are consistent with each other and agree closely with that from the fit to the normalized CASTNET data (68.5 ± 1.5 ppb). The one exception is the Rocky Mountain NP site; the ODV temporal changes at this site are consistent with those of CASTNET data but give a larger a-parameter value (73 ± 5 ppb), which is possibly due to the relatively higher elevation of the Rocky Mountain NP site (2.7 km elevation), compared with the lower elevation of the Denver urban area (~ 1.8 km elevation), and/or to the influence of Denver area urban pollution, which has been demonstrated to impact this site (Evans and Helmig, 2017). The

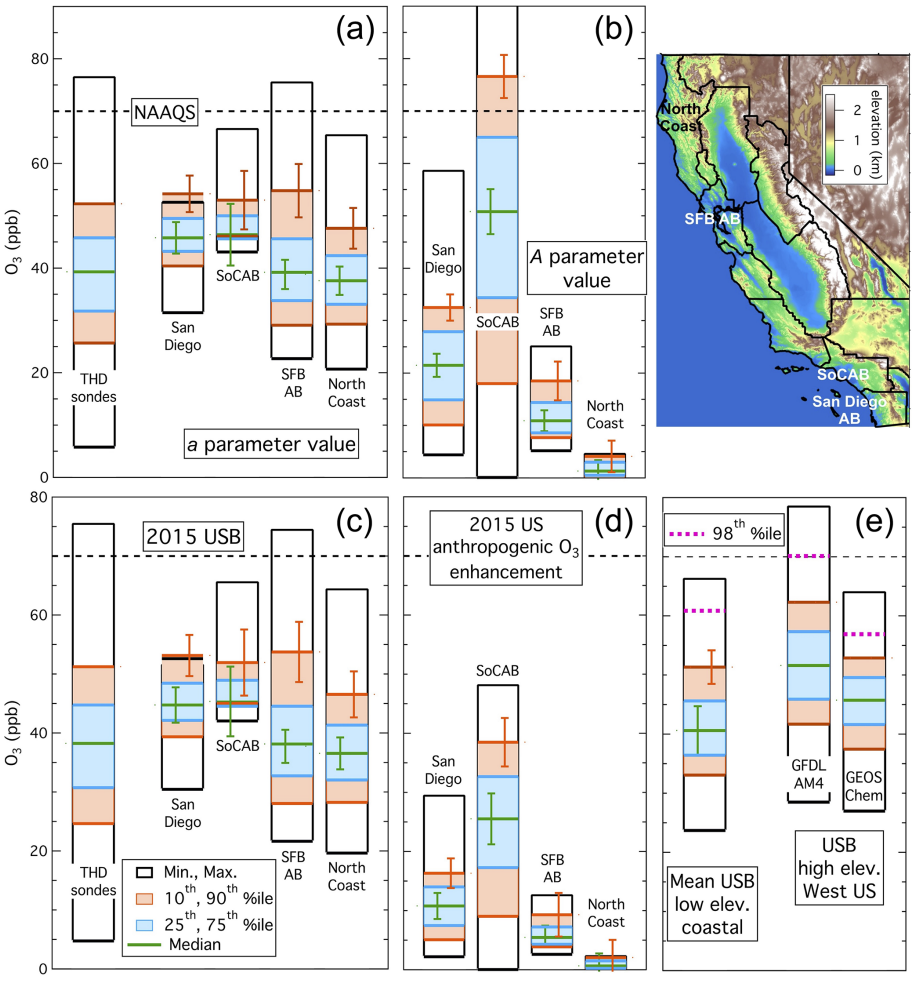

Figure 3. Comparisons of estimates of the MDA8 ozone component distributions in four coastal Californian air basins; the inset map identifies the four air basins, with the black lines indicating air basin boundaries. **(a)** Comparison of ozone concentrations measured between 0.6 and 1 km altitude by sondes launched from Trinidad Head (THD) from May through September from 1997 to 2017 and derived *a*-parameter values. **(b)** Comparison of derived *A*-parameter values. **(c)** Comparison of the same sonde ozone measurements and the year 2015 USB distribution. **(d)** Comparison of the year 2015 distributions of US anthropogenic enhancements. **(e)** Comparison of the mean of the 5-year 2015 USB distributions illustrated in panel **(c)** with the distributions of the daily MDA8 USB for April–June 2017 at western US high-elevation sites simulated by two global models; these latter bar graphs were derived from Fig. 17 of Zhang et al. (2020). Error bars on the median and 90th percentile lines indicate estimated uncertainties in the determination of the USB and the US anthropogenic ozone enhancement percentiles as well as the standard deviations of the means from the five USB determinations.

derived *A*-parameter values provide estimates of the US anthropogenic ODV enhancement in the year 2000 averaged over the sites in each group: 8.0 ± 1.7 and -1.9 ± 4.4 ppb in Colorado urban and rural areas, respectively; note that this rural value is consistent with zero within the derived confidence limit. The fit of Eq. (4) to the time series of maximum ODVs (with the *a*-parameter value fixed at 69.0 ppb) gives a somewhat larger *A*-parameter value ($A_{WF} = 11.0 \pm 1.7$) and a WF-parameter value of 4.0 ± 2.5 ppb; this latter value is an estimate of the ODV enhancement due to wildfire emissions in the year 2000.

An open scientific question is the role of emissions from the oil and natural gas industry and agricultural activities in elevating ODVs in the Denver urban area. To the extent that emissions from these sectors have increased similarly to wildfires, any such role would contribute to our derived WF-parameter value, which is larger in the Denver urban area than in other urban areas considered here (see Table S4). With a different temporal dependence, they could bias the derived *a*-parameter value; however, the good agreement between that estimate in the Denver urban area, rural Colorado and the CASTNET data indicates no more than a small bias.

Figure 6 shows the results of similar analyses for six other southwestern US urban areas. In these plots (and in Fig. S2), the black, generally lower curves with dashed extensions are the fit to the baseline data from Fig. 1, normalized to the re-

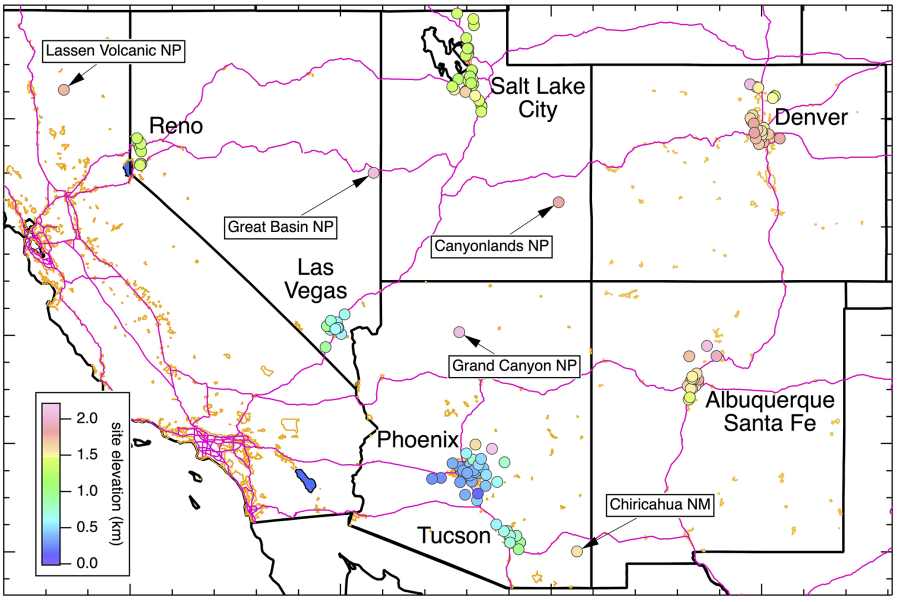

Figure 4. Map of southwestern US urban monitoring sites; the symbols are color-coded according to site elevation, as indicated in the annotation. Lines indicate the outlines of southwestern US states (black), urban areas (gold), and interstates and other selected major highways (violet). Seven urban areas, whose sites are analyzed together as separate data sets, are labeled. The locations of five of the isolated rural CASTNET sites are also included.

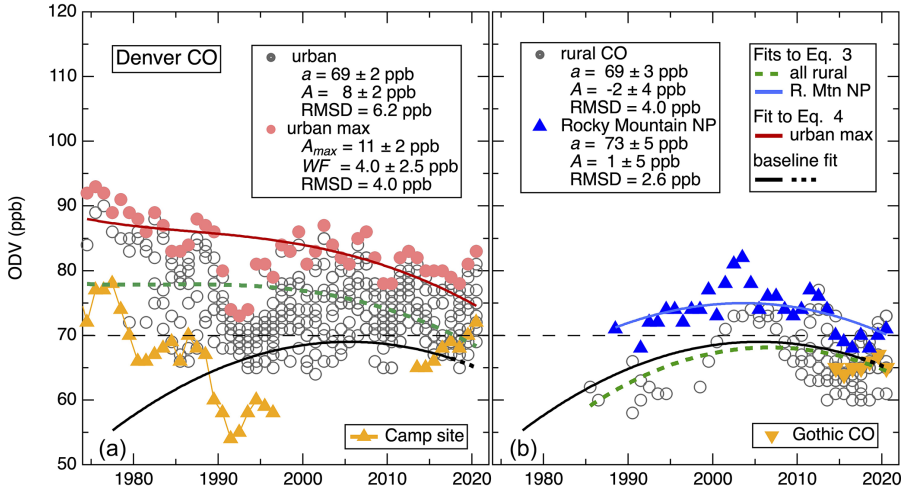

Figure 5. Time series of ODVs recorded in Colorado **(a)** at the urban sites whose locations are shown in Fig. 4 and **(b)** at rural sites (excluding the Four Corners area) whose locations are shown in Fig. S1. Open symbols indicate all ODVs recorded in each area, and solid symbols indicate ODVs from three specific sites and the maximum Denver urban ODVs. As indicated by the annotation in panel **(b)**, dashed green curves indicate fits of Eq. (3) to all plotted ODVs (excluding the Camp and Rocky Mountain NP sites), the blue curve in panel **(b)** indicates the Rocky Mountain NP fit of Eq. (3), and the solid red curve in panel **(a)** indicates fit of Eq. (4) to the maximum Denver urban ODVs; parameters derived in these fits are annotated in the graphs. The solid black curves with dashed extensions indicate the fit to the baseline data included as the gray curve in Fig. 1. The light dashed lines indicate the 70 ppb ozone NAAQS threshold value.

spective a-parameter values; thus, these curves indicate the temporal behavior of ODVs in each data set that would have been expected in the absence of US anthropogenic emissions. The derived a-parameter values are similar in five of those areas, all falling in the range of 66.2–69.0 ppb, and agree well with the Denver (69.0 ± 2.1 ppb) and CASTNET (68.5 ± 1.5 ppb) results discussed above. Only in Tucson is a significantly smaller a-parameter value (63.9 ± 1.4 ppb) derived; this value is also smaller than that found at the nearby Chiricahua NM CASTNET site (70.1 ± 1.7 ppb). The lower elevation of Tucson may contribute to this difference. Fits of Eq. (3) to all of the rural ODV time series (Fig. S2

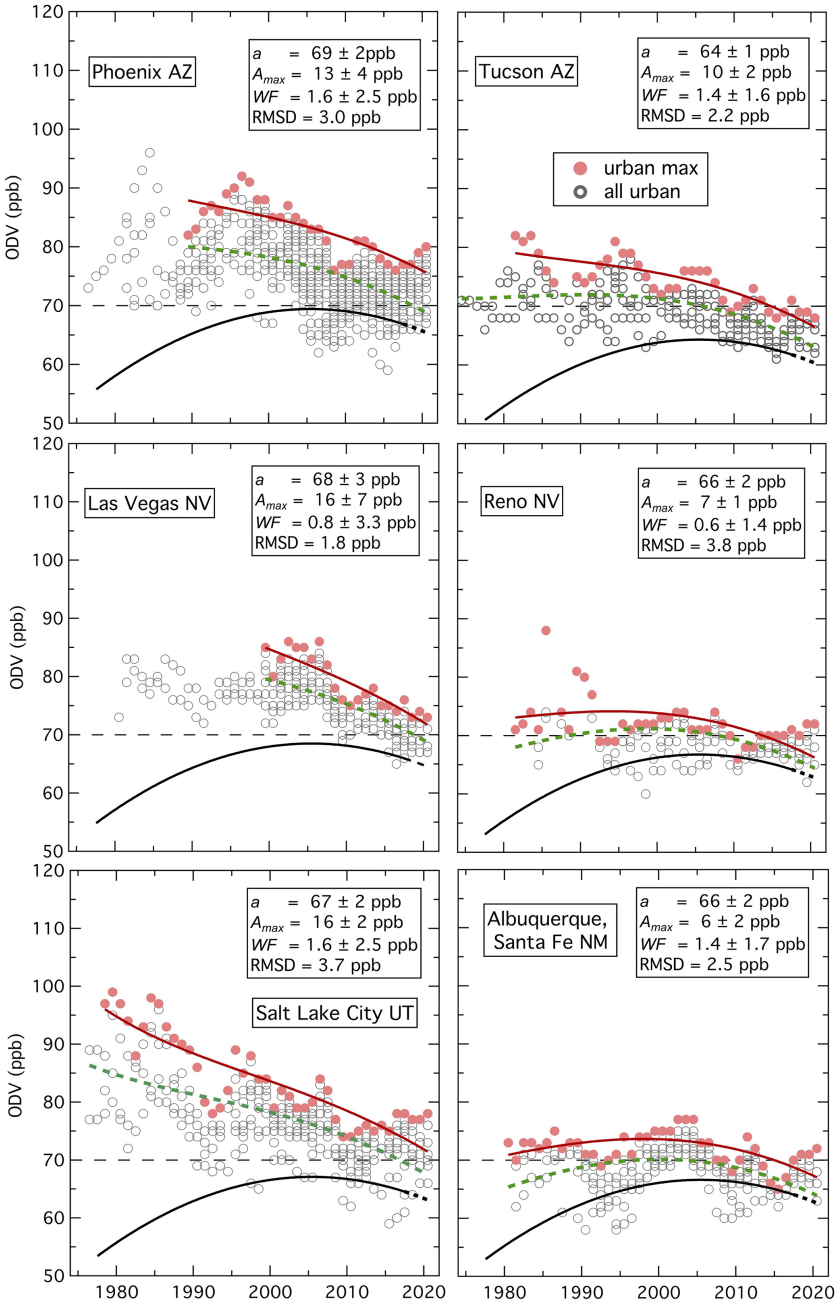

Figure 6. Time series of ODVs recorded in six southwestern US urban areas shown in Fig. 4. Open symbols indicate all ODVs recorded in each area, while solid symbols indicate the maximum ODVs in each year in each area. As in Fig. 5, dashed green curves indicate fits of Eq. (3) to all ODVs, whereas solid red curves indicate fits of Eq. (4) to the maximum ODVs, with the parameters derived in this fit annotated. The solid black curves with dashed extensions indicate the fit to the baseline data from Fig. 1, normalized to the respective a-parameter values. The light dashed lines indicate the 70 ppb ozone NAAQS threshold value.

and Table S3) also give similar a-parameter values (within 65–69 ppb), with small A-parameter values (−3 to +5 ppb). Fits of Eq. (4) to the maximum urban ODVs (with the a-parameter values fixed at the values derived from the ODVs in the entire respective urban area) give A_{WF}-parameter values in the range of 6–16 ppb. Small, positive wildfire ODV enhancements (WF range of 0.6–1.6 ppb) are derived in all six urban areas, although the confidence limits of all include zero.

In summary, analyses of the ODV time series throughout the southwestern US give remarkably consistent results. The weighted average a-parameter value, which gives an es-

timate of the US background ODV in the year 2000, derived from 11 urban and rural ODV time series, is 67.4 ± 0.7 ppb, with only the low-elevation, most southerly Tucson urban area giving a significantly lower value; this average agrees well with the value derived in the CASTNET site analysis (68.5 ± 1.5 ppb). This overall agreement indicates that an approximately constant, common US background ODV value is found throughout the southwestern US. The mean A-parameter value, which gives an estimate of the US anthropogenic ODV enhancement, derived from four rural ODV time series, is -0.1 ± 2.9 ppb, which indicates that ODVs outside of urban areas are little affected by US anthropogenic emissions throughout this entire region. Any area with intense agricultural activity may be an exception to this general finding, due to the influence of uncontrolled anthropogenic emissions from this activity. Within the seven urban areas, the A_{WF} values span the range from 6 to 16 ppb, with the larger values (11–16 ppb) derived in the four nonattainment areas. Wildfire emissions contribute additional ODV enhancements within urban areas: estimated as 0.6–4.0 ppb (mean of 1.6 ± 0.9 ppb) in the year 2000 and 1–6.4 ppb (mean of 2.6 ± 1.4 ppb) in 2020.

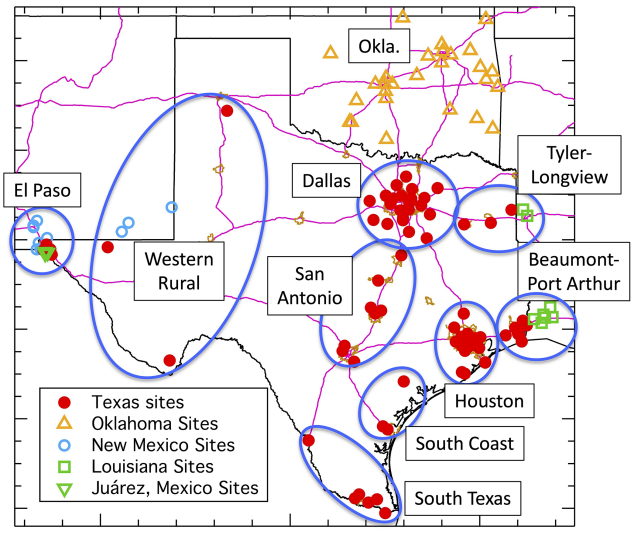

Figure 7. Map of monitoring sites within the Texas region; the symbols are color-coded according to state, as indicated in the annotation. Lines indicate outlines of southwestern US states (black), urban areas (gold) and interstates (violet). Nine Texas regions, whose sites are analyzed together as separate data sets, are indicated.

4.4 ODV contributions in Texas

The ozone monitoring site locations throughout Texas as well as those in some sites in neighboring states are indicated in Fig. 7, which also identifies the division of these sites among nine Texas regions and the state of Oklahoma; we examine the ODVs recorded in these regions. Figure 8 plots the ODV time series recorded in seven of the nine Texas regions, and Figs. S3 and S4 give similar plots for the other two Texas regions, for Oklahoma and for eight additional surrounding states. The parameter values derived from fits of Eqs. (3) and (4) to all ODV time series are annotated in the figures and given to greater precision in Tables S4 and S5. In Fig. 8 and in the upper graphs of Fig. S3, the ODVs for the entire state of Texas (gray symbols) are included in the plots highlighting the regional ODVs (colored symbols), which are fit to Eq. (3), as indicated by the upper black solid curves. The lower black curves with dashed extensions indicate the fit to the baseline data from Fig. 1, normalized to the respective a-parameter values; these curves indicate the temporal behavior of ODVs in each region that would have been expected in the absence of US anthropogenic emissions.

Comparison between Figs. 6 and 8 (note differences in the ordinate scale) indicates that ODVs in Texas were often much larger in earlier decades than those in the southwestern US urban areas, indicating much larger impacts from US anthropogenic emissions in Texas. For example, the maximum US anthropogenic ODV enhancements (i.e., A_{WF}-parameter values) in Texan urban areas in the year 2000 were generally > 25 ppb, while they were as high as 54 ± 3 ppb in the Houston region, compared with the range of 6–16 ppb found in the southwestern US. However, the ODVs in Texas have decreased by a larger absolute amount than in the southwestern US; thus, at present, the maximum ODVs in Texas are no larger than those in the Denver and Phoenix urban areas.

The southwestern US is characterized by an approximately constant US background ODV across the entire region; however, there is a pronounced spatial gradient across Texas. The a-parameter values of 65 ppb derived for the El Paso and western rural regions are similar to the weighted mean (67.4 ± 0.7 ppb) of the urban and rural southwestern a parameter. However, the US background ODV decreases with distance both east and south across the state, with the smallest values found in southern and eastern Texas – 50 ± 5 ppb in southwestern Texas and 54 ± 3 ppb in Houston – which is heavily influenced by the transport of maritime air from the Gulf of Mexico (Berlin et al., 2013) during the warm (ozone) season. This broad geographic feature in USB has also been seen in several modeling studies (e.g., Fiore et al., 2014; Zhang et al., 2020).

As expected, the largest Texas US anthropogenic ODV enhancements (27–54 ppb in 2000) have generally been found in the nonattainment areas within the state – Houston, Dallas and San Antonio – although comparably large A-parameter values (28–37 ppb) are found throughout southeastern and eastern Texas. It is notable that the El Paso region is anomalous: although the A-parameter value (11 ± 2 ppb) is comparatively modest, the a-parameter value (65 ± 2 ppb) is so large that even the relatively small US anthropogenic ODV enhancement is sufficient to produce ODVs that routinely exceed the 70 ppb NAAQS threshold value throughout the entire measurement record (upper left graph in Fig. 8).

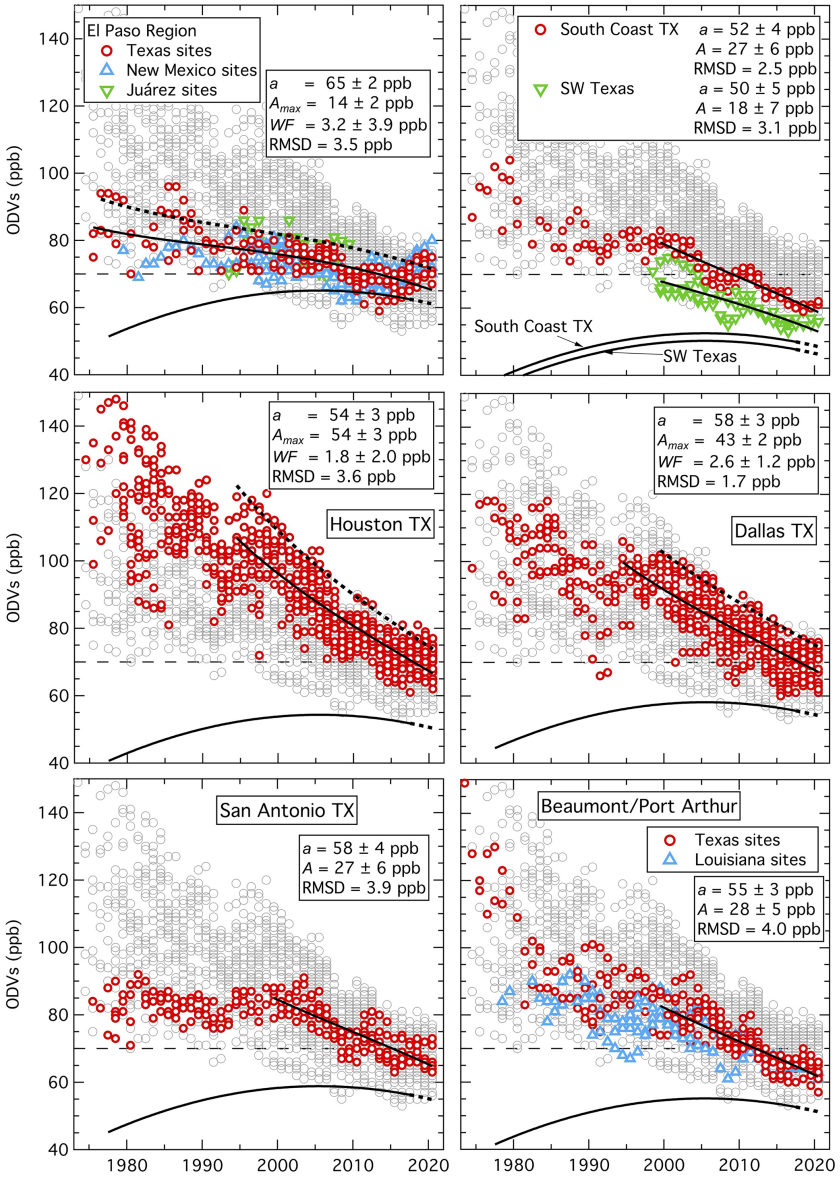

Figure 8. Time series of ODVs recorded in seven of the Texas regions shown in Fig. 7. Gray symbols in each graph indicate all recorded Texas ODVs. Colored symbols indicate the ODVs from each respective region. Upper solid black curves indicate fits of Eq. (3) to all ODVs in the area over the curve's time span; the parameters derived in these fits are annotated in three graphs; dotted curves indicate fits of Eq. (4) to the maximum ODVs in El Paso, Houston and Dallas, with the parameters derived in these fits annotated. Lower solid curves with dashed extensions indicate the fit to the baseline data from Fig. 1, normalized to the respective a-parameter values. The light dashed lines indicate the 70 ppb ozone NAAQS threshold value.

There is evidence that the maximum ODVs in Texan urban areas may be elevated by ozone sources that have not yet been effectively controlled by air quality improvement efforts. Such sources could possibly include wildfire emissions, which are approximately quantified by Eq. (4), or emissions from oil and gas exploration and production, which are ubiquitous across Texas. To gauge the possible magnitude of these sources, Eq. (4) is fit to the time series of maximum ODVs in Dallas and Houston (dotted black curves in the middle graphs of Fig. 8). These fits possibly indicate contributions of 2–3 ppb to the maximum ODVs in these urban areas from such growing, uncontrolled anthropogenic sources. Iglesias et al. (2022) show the significant growth in wildfires across all of Texas (their Fig. 2), especially since the turn of the century, and Gong et al. (2017) calculate that wildfires impact Houston on 3.5 % of the days in their May–September 2008–2015 study period, with an average contribution of ∼ 8.5 ppb.

4.5 ODV contributions in neighboring and more distant states

For context, preliminary analyses have been conducted of the ODV time series recorded in states lying east and north of the region that is the focus of this study. Figures S3 and S4 illustrate the results of these analysis for Oklahoma, Louisiana, Arkansas, Nebraska and Kansas; Eq. (3) is fit to the time series of all ODVs recorded in each state without consideration of intrastate regional differences. Nevertheless, the RMSDs of the ODVs about the fits are similar to the fits to more carefully selected sets of sites discussed in the preceding sections. The results for these states are considered to be adequate for determining boundary conditions for the ODV component determinations in the region that is the focus of this work.

Figure S3 also includes analyses of ODVs recorded in four rural northern states: Montana, North and South Dakota, and Wyoming. A fit to all ODVs recorded in these four states gives a mean A-parameter value of 1.3 ± 1.7 ppb, which indicates only small US anthropogenic ODV enhancements throughout that region. (Note that the Boulder site in Wyoming – AQS Site ID 56-035-0099 – reports anomalously large ODVs; as this site is in the Upper Green River basin where high ozone concentrations are produced in wintertime from the region's large oil and gas production activities (Schnell et al., 2009), all ODVs from this site have been excluded.) Separate fits of Eq. (3) to the ODV values in each state provide separate a-parameter values; there are some small differences in these results: a maximum in Wyoming of 64 ppb, a minimum in Montana of 59 ppb, and intermediate values of 60 and 62 ppb in North and South Dakota, respectively. Parrish and Ennis (2019) and Parrish et al. (2022) present earlier analyses for three of these states and found results consistent with this updated analysis.

Figure S6 includes analyses using fits of Eq. (4) to the time series of maximum ODVs recorded in the New York City and Atlanta urban areas. The New York City time series was originally analyzed by Parrish and Ennis (2019) (see their Fig. S4); here, that time series is extended through 2021. Figure S6 includes separate symbols for the Atlanta, coastal and inland sites.

5 Discussion and conclusions

5.1 Background ozone dominates observed concentrations throughout the US

Five estimates of the May to September USB distribution derived from the analysis of observations from Californian western coast locations are compared in Fig. 3c. The first bar illustrates the ozone distribution measured between 0.6 and 1.0 km altitude by sondes launched from a coastal site at Trinidad Head (Oltmans et al., 2008), which is located in the North Coast AB shown on the map in Fig. 3; Parrish et al. (2022) fully describe this data set. The ozone altitude gradient (see Fig. 1 of Parrish et al., 2022) indicates that this altitude range includes the marine boundary layer–free-troposphere transition, so that it is high enough to avoid continental influences as air is transported ashore and low enough to well-characterize air mixed into the convective boundary layer over the continent (Parrish et al., 2010). Thus, these sonde data provide direct estimates of USB concentrations. The other four bars show estimates of the distribution of USB ozone derived in Sect. 4.2 from the MDA8 distributions in Californian coastal air basins. There is reasonable agreement between the five estimates, although with some notable differences. The two southern estimates (San Diego AB and SoCAB) are somewhat larger than the three more northerly estimates, which is consistent with the systematic decrease in USB with latitude quantified by Parrish et al. (2022). Variation in site elevations also contributes to these differences. The Crestline site at 1.4 km and the Alpine site at 0.6 km are included in the SoCAB and San Diego AB, respectively; they are at higher elevations than other coastal air basin sites and very often record the largest MDA8 ozone concentrations in their respective ABs. Thus, at least some of the quantitative differences in the bars in Fig. 3c represent real atmospheric differences. The mean of all five USB distributions from that graph is included in Fig. 3e; it provides an estimate of the average USB distribution along the Californian coast.

Comparison of the distributions in Fig. 3c, d and e shows that the distribution of USB was larger than the distribution of the US anthropogenic ozone enhancements in all four Californian coastal air basins by 2015. This dominance of background ozone is quite pronounced; only in the SoCAB and San Diego AB do the distributions in Fig. 3d overlap at all with the mean USB distribution in Fig. 3e. In the SoCAB, the 75th percentile of the US anthropogenic ozone enhancement is smaller than the 10th percentile of the mean USB contribution. Comparisons for the separately derived air basin USB distributions between Fig. 3c and d shows that the USB dominance in the SoCAB and San Diego AB comparisons are even more pronounced. This predominance of the background contribution developed relatively recently; Fig. 3a and b show the comparison for the year 2000, when the US anthropogenic enhancements were generally greater than or equivalent to the USB contributions in the SoCAB and more closely comparable in the San Diego AB.

The predominant contribution of USB to maximum ozone concentrations, even in the SoCAB where the largest US ozone concentrations occur, emphasizes the great difficulty of achieving accurate air quality modeling. Traditionally, CTMs have primarily focused on careful, detailed treatment of transport and photochemical processes on local to regional scales, which is required for the accurate simulation of the US anthropogenic ozone enhancements; however, less attention has been paid to the USB contributions, especially the day-to-day variability. Of great importance for present-

day exceedance event modeling or daily air quality forecasts is the accurate simulation of USB on short-term (i.e., daily or even hourly) timescales. As USB is driven by a manifold of processes occurring on small spatial scales but over hemisphere-wide distances, accurate, detailed simulation of the stratospheric and tropospheric contributions to USB and modeling for predictions of future baseline ozone are each beyond the capabilities of current air quality models. These issues are explored in two recent comparisons of estimates of background ozone and their impacts on the simulation of surface ozone across the continental US (Hogrefe et al., 2018; Zhang et al., 2020) where background concentrations were shown to differ by 5–10 ppb in the mean and up to 15 ppb for domain-averaged MDA8 values. Figure 3e illustrates the differences between two different model simulations of the US background MDA8 ozone distributions for April–June 2017 at 12 high-elevation sites in the western US. As Zhang et al. (2020) note, the means of the distributions agree within 6 ppb. However, the larger percentiles of the distribution differ more widely; e.g., the 98th percentiles are $\sim$70 and $\sim$57 ppb from the GFDL-AM4 and GEOS-Chem models, respectively. It is notable that the former model indicates that USB alone can exceed the 2015 NAAQS threshold value of 70 ppb, while the latter model finds that USB always remained significantly below the NAAQS threshold.

5.2 Pronounced shift in the spatial distribution of maximum US ozone concentrations

Great efforts have been made over the past half-century to reduce anthropogenic precursor emissions throughout the entire country. These efforts have been remarkably successful, yielding substantial reductions in the number and magnitude of US ozone NAAQS exceedances; however, progress has not been spatially uniform over the country. Figure 9 illustrates one measure of this progress. During the 5-year period from 1997 to 2001, the large majority (43) of the 51 US states plus the District of Columbia recorded at least one ODV of 75 ppb or larger; 20 years later, during the 2017–2021 period, the number of such states had been reduced to 20. In the earlier period, 80 % of ODVs across the nation were $\geq$ 75 ppb, whereas that percentage had dropped to 10 % in the later period, clearly demonstrating a remarkable improvement in air quality with respect to ozone. However, there are marked regional differences in the percentages of ODVs $\geq$ 75 ppb: 88 % and 64 % in the eastern and western regions in the earlier period, respectively, but corresponding values of 2.4 % and 22 % in the later period. In Fig. 9 the solid blue bars in the western region demonstrate that nearly all of the seven total states that recorded more than 7 % of ODVs $\geq$ 75 ppb were in the southwestern US, including Texas and California; the single exception is Connecticut, where the maximum ODVs are recorded near the coast of Long Island Sound (Parrish and Ennis, 2019). Similar conclusions are reached if ODVs > 70 ppb are considered (Fig. S5). In summary, great improvement in US ozone concentrations have occurred over past decades, but this improvement has been accompanied by a marked shift in the highest observed ozone concentrations from the eastern to the southwestern US.

The occurrence of only modest ODV decreases in the southwestern US has been noted in other analyses. Simon et al. (2015) found that the upper end of the summertime urban ozone distribution (i.e., representative of ODVs) generally decreased over the 1998–2013 period throughout the US in response to decreasing emissions of NO_x and volatile organic compounds (VOCs). They interpreted those results as demonstrating the large-scale success of US control strategies. However, their Fig. S12 shows that the Denver urban area was an exception to this generality, with all sites exhibiting either positive or insignificant trends. Similarly, Abeleira and Farmer (2017) found that ozone in the Denver urban area was either stagnant or increasing between 2000 and 2015, despite substantial reductions in NO_x emissions. In Colorado Springs, approximately 100 km south of Denver, Flynn et al. (2021) found that summertime MDA8 ozone shows no significant trend throughout its distribution over the past 20 years. Further, they found little evidence of local photochemical production or ozone transport from Denver, consistent with our classification of this area as rural. The results of these three studies are consistent with the long-term ODV changes in urban and rural Colorado shown in Fig. 5 and with our conclusion that the US background ODV is the dominant contributor to ODVs.

5.3 Spatial and temporal distribution of ODV contributions

The derived spatial distributions of the two major ODV components – the US background ODV and the US anthropogenic ODV enhancement – are illustrated for the year 2000 as contour maps in Figs. 10 and 11, respectively. In Fig. 10, the estimated US background ODVs are at a maximum – greater than 64 ppb (see violet contour) – throughout the entire southwestern US, including western Texas and Wyoming, and above 68 ppb in some areas, including most of Colorado. We attribute these large values to baseline air at higher altitudes flowing over the inland mountain ranges and mixing into the convective boundary layer over the continent (Langford et al., 2017). The overall spatial pattern is similar to those simulated for surface impacts of ozone transport from Asia (see Fig. 9 of Lin et al., 2012a), stratospheric intrusions (see Fig. 11 of Lin et al., 2012b) and USB distributions (see Fig. 1 of Zhang et al., 2020). Previous studies of reanalysis data sets (Sprenger and Wernli, 2003; Škerlak et al., 2014) have described the southwestern US as being prone to high rates of transport from the deep stratosphere to the troposphere. These events tend to cross the tropopause at high latitudes (40–60° N) near the end of the North Pacific storm track but make their surface impacts felt most acutely after quasi-isentropic subsiding transport to the southeast (in

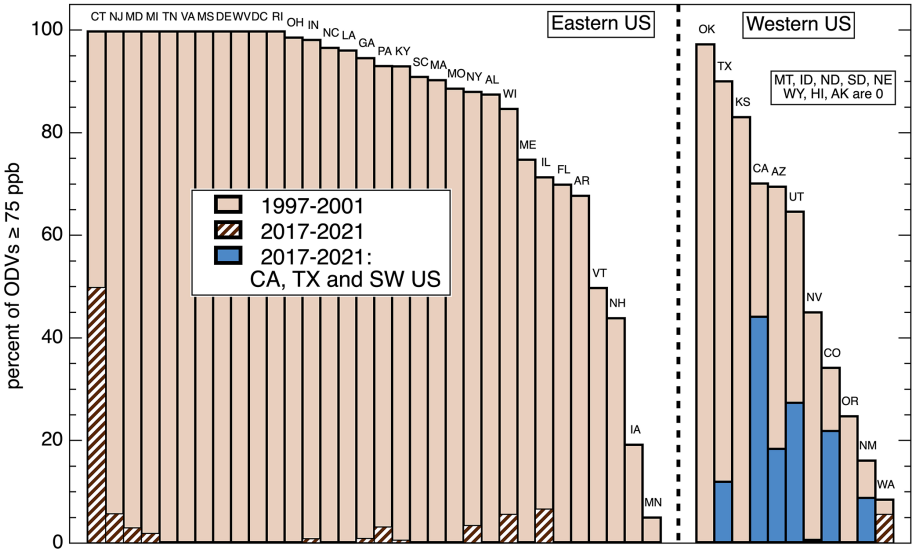

Figure 9. Comparison of the percentage of ODVs greater than or equal to 75 ppb recorded at all sites in individual states over two 5-year periods: 2017–2021 (hatched and dark-blue bars) and a period 20 years earlier – 1997–2001 (light-colored bars). Individual states are indicated by their two-letter abbreviations (defined in Table S6). States are arbitrarily divided between eastern and western regions. Southwestern states, Texas and California are indicated by solid dark-blue bars. Eight rural states, all in the western region, reported no ODVs greater than or equal to 75 ppb in either period.

the lee of the Pacific High). While the peak of this effect occurs in the spring, it does continue into the summer (Škerlak et al., 2014), when it can more strongly couple with the surface because of the very deep convective boundary layers that develop in the arid, high terrain of the southwestern US. With such large US background ODV values, even relatively small anthropogenic enhancements in the regional urban areas raise ODVs above the 70 ppb ozone NAAQS threshold, thereby leading to their designation as nonattainment areas. Were the NAAQS threshold to be lowered further, for example, to 65 ppb, as has been considered in the past (e.g., Regulatory Impact Analysis of the Final Revisions to the National Ambient Air Quality Standards for Ground-Level Ozone), Fig. 10 indicates that NAAQS achievement would be precluded over the vast southwestern US region inside the 64 ppb contour (unless regulatory efforts could reduce the US background ODV). A striking feature of the contour map in Fig. 10 is the significant spatial gradient in the US background ODV over the continent. Increases occur inland from the western coast as surface elevations increase (Parrish et al., 2022), with decreases to the north and east of the broad maximum in the southwestern US and to the east and south within Texas. These smaller values in eastern Texas (e.g., 54 ± 3 ppb in Houston) allow for larger anthropogenic ODV enhancements there before the NAAQS threshold is exceeded.

CTMs have been extensively utilized to estimate US background ODVs. Figure 10 compares our observation-derived results with a portion of Fig. 3 of Jaffe et al. (2018), who presents the results of a simulation by the GFDL-AM3 model of a statistic comparable to the US background ODV. The broad spatial features are similar in both plots; the maximum in the southwestern US is the dominant feature in each. The maximum observation-derived values (68–70 ppb) are consistent with the model-simulated maximum (60–70 ppb). All of the observation-derived values, except for a narrow band along the Pacific coast, are in the 50–70 ppb range, as are the model-derived values, with the exception of the values in the southeast corner of that map. Both results show general south-to-north and west-to-east decreases in inland US background ODVs. However, it is apparent that the observation-based estimate has substantially greater precision and spatial resolution compared with the low-resolution ($200 \times 200\,km^2$) model estimate. Jaffe et al. (2018) estimate that the model uncertainty in the seasonal mean USB is $\sim \pm 10$ ppb, although it is larger for individual days, such as is required for the determination of US background ODVs. The magnitudes of the model- and observation-derived results in Fig. 10 agree within this estimated uncertainty in the model simulations. The US background ODV estimated from the GFDL-AM4-simulated ozone distribution (approximated by the 98th percentile) shown in Fig. 3 is also consistent with the contour map in Fig. 10, indicating that US background ODVs above 68 ppb over the southwestern US are indeed physically realistic.

The NO_2 column measurements from the Ozone Monitoring Instrument (OMI) satellite (Lu et al., 2015) are included in Fig. 11 for comparison with the US anthropogenic ODV enhancements, which, outside of California, are generally elevated in the larger southwestern US and Texan ur-

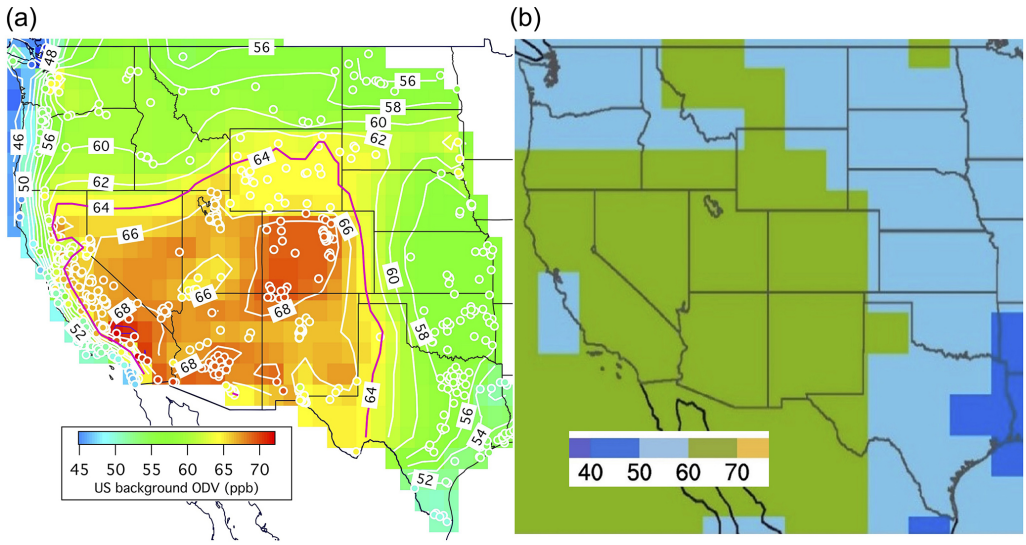

Figure 10. Two estimates of the spatial variability in US background ODVs over the western US. **(a)** Contour map of estimated US background ODV for year 2000. The US background ODV excludes estimated wildfire contributions. The 64 ppb contour is colored violet to indicate the extensive area of the largest values. Symbols in the contour map indicate individual monitoring sites included in the analysis with the same color coding as the contour map. Results from Parrish et al. (2017, 2022) and estimates for California's Central Valley (Faloona et al., 2025) are included. **(b)** Annual fourth-highest MDA8 ozone concentration averaged over 2010–2014, from a GFDL-AM3 model simulation with North American anthropogenic emissions zeroed out (figure reproduced from a section of Fig. 3 of Jaffe et al., 2018).

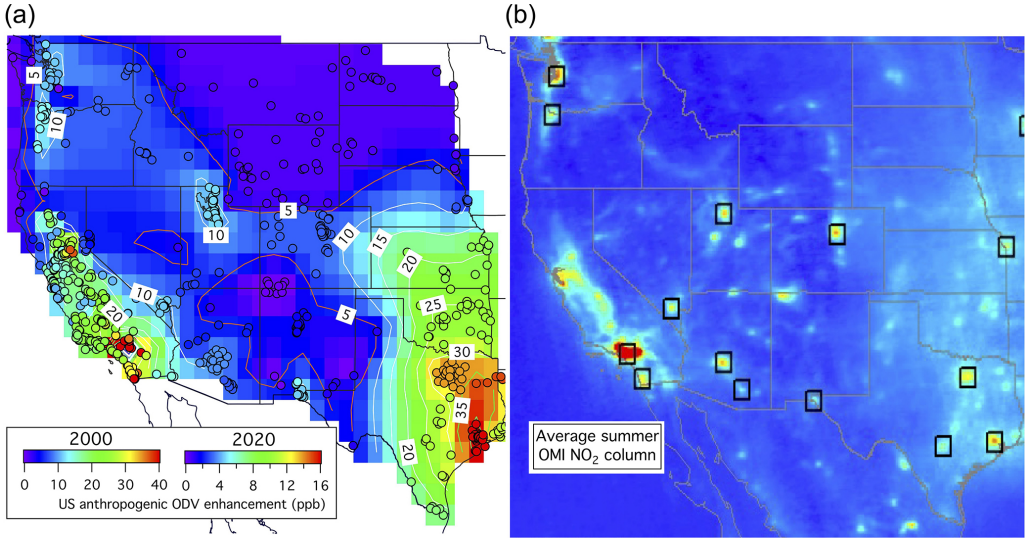

Figure 11. US anthropogenic ODV enhancement over the western US compared to mean summertime OMI NO_2 columns. **(a)** Contour map of estimated US anthropogenic ODV enhancement for the year 2000 over the western US. Symbols on the contour map indicate individual monitoring sites included in the analysis with the same color coding as the contour map. A second color scale is included for interpretation of the colors as the year 2020 US anthropogenic ODV enhancement. Results from Parrish et al. (2017, 2022) and estimates for California's Central Valley (Faloona et al., 2025) are included. **(b)** The OMI NO_2 columns measured in April–September 2005–2014 are reproduced from Fig. 1a of Lu et al. (2015) by cropping and changing the aspect ratio of that figure to approximate that of the contour map.

ban areas. There is general correlation of the NO_2 columns within these urban areas, which supports our interpretation of the derived *A*-parameter value as quantifying the US anthropogenic ODV enhancement. However, some areas of clear differences between these ODV enhancements and the OMI NO_2 column measurements are evident in Fig. 11. Most clearly, emissions from the large coal-fired power plants in the Four Corners region (location identified in Fig. S1) give a strong elevation in the NO_2 column that is not reflected in US anthropogenic ODV enhancements. This lack of corre-

lation is consistent with the ODV time series for this region (Fig. S2), which indicates that the US anthropogenic ODV enhancement is near zero. Mesa Verde NP is in this region; it has been considered a high-elevation site representing baseline O_3, at least in the spring, by Lin et al. (2017). This site records ODVs generally consistent with all other sites in this region. The co-location of the large NO_2 enhancement with an indiscernible US anthropogenic ODV enhancement indicates that the large NO_2 emissions from the power plants have only a negligible effect on the regional ODVs. The Denver urban area, with *A*-parameter values in the 8–11 ppb range (Fig. 5), does not stand out in Fig. 11, although that area does have a clear signature in the OMI NO_2 column data.

Figure 12 compares the long-term changes in the ODV components between the Crestline site in the Los Angeles urban area with those in the four larger southwestern US urban areas and three Texan urban areas. Since $\sim$1990, the Crestline site has usually recorded the largest ODV in the SoCAB. Overall, decreases in ODVs have been recorded in each of the eight cities; this decrease is primarily driven by a decrease in the US anthropogenic ODV enhancement. The final term in Eq. (3) indicates that this contribution decreased by a factor of 6.3 between 1980 and 2020. In contrast, the first three terms of Eq. (3) indicate that the US background ODV increased by $\sim$11 ppb over the entire western US region from 1980 to the mid-2000s and has since slowly decreased. The relatively minor but increasing (up to $\sim$6 ppb in Denver in the year 2020) mean ODV enhancements due to wildfire emissions are separately indicated. Two conclusions emerge from Fig. 12. First, throughout the monitoring record, the US background ODV has been, by far, the largest ODV contribution in the four southwestern US urban areas; moreover, by 2000, it had become the predominant ODV contribution in all cities, even within the Los Angeles urban area exemplified by the Crestline site. This conclusion is consistent with the discussion in Sect. 5.1. Second, the increase in the US background ODV between 1980 and the mid-2000s and the increasing wildfire contribution through the entire period partially offset the reduction in the US anthropogenic ODV enhancement, so that ODVs have not changed greatly in the southwestern US urban areas and El Paso, Texas.

There are some notable deviations from the overall picture described above. First, the results shown in Fig. 12 and all fitted curves in all figures represent the average behavior of the fitted ODVs; there is significant scatter about those fits as quantified by the RMSDs (generally < 5 ppb) annotated in the figures and given in Tables 1, S1 and S3–S5; this scatter appears to be predominately year-to-year variability. However, one systematic deviation – the recent anomaly of the El Paso nonattainment area and nearby rural New Mexico (see graphs in Figs. 8 and S3) – is particularly relevant; the ODVs in the last few years are as much as 15 ppb larger than expected from the fits to Eq. (3). It is notable that, in the most recent year included in this analysis (2021), the largest ODV (80 ppb) in the two-state region of Texas and New Mexico was not recorded in either of the traditional urban ozone hot spots of Houston or Dallas; rather, it was recorded at the rural Desert View site in New Mexico, which is included in the El Paso region in Fig. 8. Only a single site in Phoenix within the entire southwestern US and Texas region (excluding California) equaled that ODV. ODVs nearly as high were recorded at rural New Mexico sites that are included in the western rural Texas region in Fig. S2. The cause of these high ODVs is presently unexplained, although it may be important to note that these regions are in the Permian oil and gas basin (Karle et al., 2021).

5.4 Implications for US air quality policies

This spatial difference in the success of air quality policies aimed at ODV reduction has resulted in a pronounced regional shift in the occurrence of ODVs of 75 ppb and above (and above 70 ppb; Fig. S6), with a growing preponderance of the nation's largest ODVs recorded in the southwestern US (see discussion in Sect. 5.2). The cause of this change is clear in Fig. 10: the southwestern US suffers from large US background ODVs that closely approach the NAAQS threshold values. In Fig. 12, it can be seen that the US anthropogenic ODV enhancements in the southwestern US urban areas and El Paso, Texas, have been reduced in magnitude to such an extent that all were smaller than 6 ppb by 2020. However, even these remaining enhancements are large enough to raise the recorded ODVs above the 70 ppb 2015 NAAQS threshold as well as the 75 ppb 2008 NAAQS threshold. This conclusion is further illustrated in Fig. 13, where fits of Eq. (4) to time series of maximum ODVs in three southwestern US urban areas are compared to similar fits in three of the largest US urban areas; additionally, the fit of Eq. (3) to the time series of CASTNET ODVs and the temporal evolution of the corresponding baseline ozone concentrations from Fig. 1 are included. In Atlanta and New York City, with substantially lower year 2000 maximum US background ODVs of 49 and 52 ppb, respectively, the fits to the urban maximum ODVs dropped below the Phoenix and Denver fits in the early 2010s; they have now dropped below the 70 ppb NAAQS threshold and are approaching the Reno, CASTNET and baseline fits. Interestingly, by 2021, the fit to the maximum ODVs recorded at all locations in Fig. 13, from the isolated rural CASTNET sites in the western US to the major metropolitan areas of Atlanta and New York City (excluding the Los Angeles), were in the 66–76 ppb range, with the southwestern US urban areas defining the upper limit. Importantly, all curves included in Fig. 13 are direct fits to measured concentrations; they do not depend upon accurate differentiation between the separate ODV contributions.

The spatial shift in the nation's highest ozone concentrations to the southwestern US emphasizes a long-standing concern with US policies for improving ozone air quality: a single standard is applied to the entire

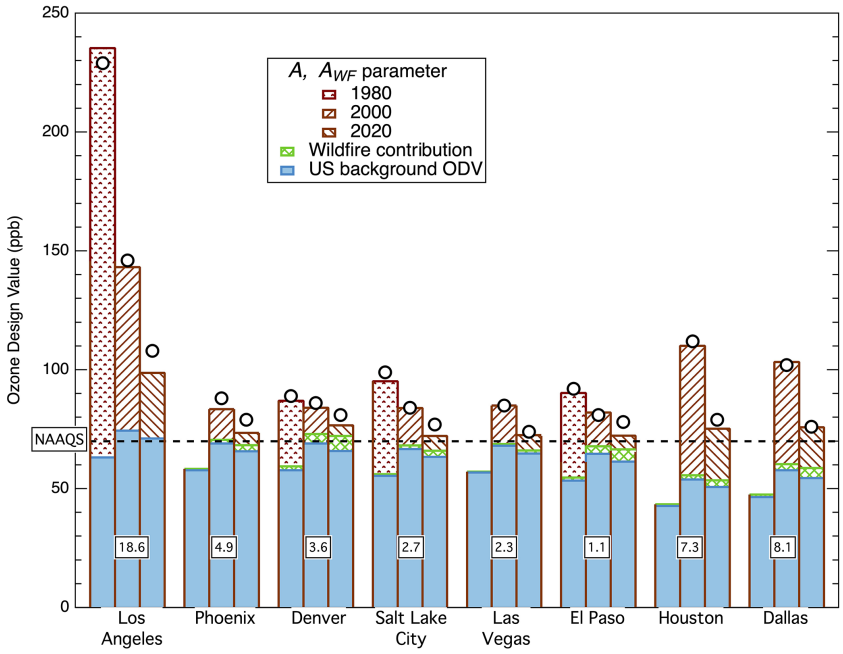

Figure 12. Derived apportionment of maximum ODVs for 3 years at 20-year intervals for the Crestline site in Los Angeles, four southwestern US regions and three Texan urban areas. The lower, solid blue bars indicate the US background ODV; they exclude estimated wildfire contributions, which are separately indicated by the middle, cross-hatched green bar segments. The top, patterned brown bars indicate the estimated US anthropogenic ODV enhancements, again excluding the wildfire contribution. For four cities, the US anthropogenic ODV enhancements and wildfire contributions are missing in 1980, as the tabulated ODVs are inadequate to estimate that parameter that early in the monitoring record. The 2020 populations of the urban areas are annotated in millions. The circles indicate the actual maximum ODVs recorded in the respective years in each area.

country without regard for the USB; this background cannot be addressed by local or regional reductions in ozone precursors. This policy contrasts with those addressing another environmental hazard – exposure to ionizing radiation. The US Nuclear Regulatory Commission (NRC, https://www.nrc.gov/about-nrc/radiation/around-us/doses-daily-lives.html, last access: 7 October 2022) estimates that about half of the average American radiation dose is due to natural background radiation that, similar to ozone, is higher in the high-altitude southwestern US. Health and safety standards for ionizing radiation are based on the additional exposure that comes from anthropogenic sources of radiation, not on the overall radiation exposure. A similar approach for ozone would require that the ozone standard be based on the anthropogenic increment of ozone above the USB within a region, rather than on the total ambient ozone concentration; alternatively, a regionally varying ambient concentration standard that accounted for the regionally varying USB could serve that purpose. Of course, such an approach would introduce additional complexity, as ozone is a secondary air pollutant that can cross state lines, making it difficult to define a suitable boundary for any particular region, such as the southwestern US. However, as of 2020, we estimate that the US anthropogenic ODV enhancement in eight southwestern US urban areas (the seven in Fig. 4 plus El Paso TX) has been reduced to the range of 2.4–6.4 ppb; however, the US background ODVs plus the relatively small wildfire contributions are so large that five of these eight cities are the centers of ozone nonattainment areas. Importantly, it is only the small US anthropogenic ODV enhancement that can possibly be directly reduced through further controls on urban and industrial emissions, although the small wildfire contributions can also possibly be reduced indirectly through decreased NO_x emissions in VOC-poor urban areas. In Denver in 2020, we estimate that the US anthropogenic ODV enhancement had been reduced to 4.4 ppb, but the US EPA has recently downgraded the Denver urban area from a Serious to Severe-15 nonattainment area under the 2008 ozone NAAQS (https://www.govinfo.gov/content/pkg/FR-2022-10-07/pdf/2022-20458.pdf, last access: 7 February 2024). This redesignation will require further reductions in local and regional precursor emissions, even though the US anthropogenic ODV enhancement is already so small that such additional emission control efforts can be expected to have little impact on future ODVs.

Importantly, it is estimated that baseline ozone concentrations at northern midlatitudes increased by a factor of 2.1 ± 0.2 between 1950 and 2000 (Parrish et al., 2021b). These baseline concentrations, which largely account for the US background ODV, reached a maximum in the mid-2000s

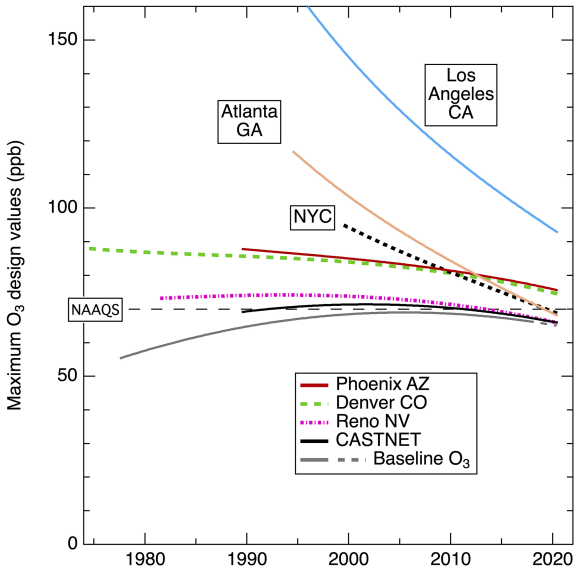

Figure 13. Comparison of fits of Eq. (4) to time series of maximum ODVs recorded in three of the nation's largest urban areas and three southwestern urban areas, with the fits to normalized rural western CASTNET ODVs and baseline ozone from Fig. 1. The fitted urban curves are taken from Fig. 2 of Parrish et al. (2022) for Los Angeles, Fig. S6 for New York City (i.e., NYC) and Atlanta GA, Fig. 5 for Denver CO, Fig. 6 for Phoenix AZ and Reno NV, and Fig. 1 for CASTNET and baseline ozone.

and have since slowly decreased at a mean rate of $\sim$ 1 ppb per decade (Parrish et al., 2020). This decrease results from decreasing anthropogenic ozone precursor emissions throughout northern midlatitudes due to the implementation of effective emission controls in North America, Europe and (more recently) East Asia. Given the large increase in baseline ozone that occurred as anthropogenic emissions increased in the 20th century, it can be expected that a significant decrease in baseline ozone can be achieved by further reducing total zonal precursor emissions. Cooperative, international emission control efforts aimed at continuing (or even accelerating) the current decrease in baseline ozone concentrations (and thereby the US background ODV) may be an effective alternative policy approach to further reducing US ODVs. It should be noted that this expectation relies on the assumption that the background will continue to decrease; however, that expectation could be compromised by the changing climate. For example, stratosphere–troposphere exchange rates could increase due to acceleration of the Brewer–Dobson circulation; modeling work by Abalos et al. (2020) points toward a 10 %–15 % rise in the stratosphere–troposphere O_3 source by the end of this century.

We should step back from the comparison of air quality policy approaches to note that there is evidence that further reductions in ambient ozone concentrations throughout the US will provide significant health benefits (e.g., Zhang et al., 2019). This applies to both attainment and nonattainment areas and to the entire concentration distribution of ozone, not just the few days of highest concentrations that determine the ODVs that are the focus of NAAQS attainment. Thus, all reductions in ozone precursor emissions will be beneficial and, if carried out in all northern midlatitude countries, will serve to further reduce baseline ozone concentrations, thereby easing the attainment of air quality standards based on ODVs or other statistics designed to quantify ozone concentrations of concern. Moreover, control measures that reduce VOC and NO_x emissions have the added benefits of reducing other criteria air pollutants, air toxics, co-emitted greenhouse gases and precursors to fine-particle formation, which contribute to haze and visibility reduction; further air quality improvement is desirable from multiple perspectives.

5.5 A required modeling hierarchy

Derwent et al. (2023) emphasize the need for a widely accepted, simple, conceptual "model" that intuitively explains the broad features of how ozone sources, sinks and transport processes all interact to establish the observed local, regional and larger-scale spatial distributions; seasonal cycles; and long-term temporal changes in ozone. Broadly speaking, this conceptual model envisages background air containing ozone and other baseline trace species entering an urban area or rural region. Urban emissions, other anthropogenic emissions and biogenic precursor emissions drive local- and regional-scale photochemical ozone production, which elevates ozone concentrations above the global baseline levels, leading to human health effects and crop and vegetation damage. After 1 to several days travel downwind, the regionally polluted air with elevated levels of ozone, other photochemical products and unreacted precursors is lofted from the continental boundary layer and rejoins the global circulation. However, neither a conceptual model nor our observation-based model applied in this paper can alone provide a quantitative understanding of tropospheric ozone; rather, a robust hierarchy of models is required.

In this regard, we believe that two key points made by Held (2005) are particularly important:

> It is fair to say that we typically gain some understanding of a complex system by relating its behavior to that of other, especially simpler, systems. For sufficiently complex systems, we need a model hierarchy on which to base our understanding, describing how the dynamics change as key sources of complexity are added or subtracted.
>
> Elegance versus Elaboration. An elegant model is only as elaborate as it needs to be to capture the essence of a particular source of complexity, but it is no more elaborate.

Emanuel (2020) makes similar points from a somewhat different perspective:

> As it becomes easier to undertake complex computer simulations of climate and weather, … it is tempting to use computers to simulate, rather than understand, nature.
>
> It is sometimes perceived as easier to run the model than to develop a comprehensive and satisfying understanding of the phenomena in question.

In addition to the conceptual model and the simple mathematical model that we apply here, comprehensive numerical models (i.e., CTMs) that aim to simulate (in full detail) as much of the atmospheric chemistry and dynamics as possible are essential to provide the beautifully detailed results that are presently available to the atmospheric community. CTMs require great "elaboration" to adequately treat the manifold of important processes, while our observation-based model is focused much more on "elegance", although it does indeed "capture the essence of a particular source of complexity". In the present work, that complexity is the interaction of USB with US anthropogenic contributions to establish observed ozone concentrations. The simplicity of our model allows a direct, conceptual understanding of the phenomena that underlie the observed ozone distribution, and this understanding provides context for the detailed results provided by CTM simulations.

From the "elaborate" perspective, it is well understood that the temporal and spatial distribution of ozone in the troposphere results from the interactions of a great many chemical and physical processes driving ozone sources, sinks and transport; fully understanding this distribution requires that the impacts of each of those processes be accurately simulated and the results be fully integrated with each other. CTMs approach this challenging task through computational parameterizations of each process in concert, with the intention of reproducing observed characteristics of the ozone distribution. It is only through successful implementations of such global CTM simulations that a full understanding of the complex reality of tropospheric ozone distribution can be achieved. However, biases in present CTM results are quite often found to be in the range of 5–20 ppb (Hu et al., 2017; Zhang et al., 2020), particularly in the extreme wings of the ozone distribution where the ODVs lie. Comparison of results between different models demonstrates that large uncertainties remain in our understanding; Sect. S1 in the Supplement briefly discusses some model result comparisons. Such comparisons have led to the increasing recognition that CTMs are not yet able to provide accurate estimates of atmospheric ozone concentrations without imposing additional constraints directly from observations. For example, Skipper et al. (2021) present a method to fuse ozone observations with USB simulated by a regional CTM in order to correct model bias, and Hosseinpour et al. (2024) present a machine learning technique that gives larger, more accurate CTM estimates of US background ODVs; this approach led to improved agreement with the Parrish et al. (2017) estimate for Los Angeles and the Parrish and Ennis (2019) estimate for New York City. Our much simpler, observation-based model takes a contrasting approach; it avoids detailed process simulation by analyzing the measured ozone distribution, which necessarily reflects the accurately integrated impacts of all relevant processes, because the atmosphere itself has performed that integration. Results of our simpler model also have significant uncertainty, which arises from the underlying assumptions required to interpret observations so as to extract information regarding the processes that produced the observed ozone distribution. In this regard, the simplicity of this model is helpful, because impacts of the model assumptions can be readily evaluated; Sects. S2–S6 in the Supplement discuss some of these evaluations. In contrast, the manifold of parameterizations that CTMs require to simulate the many relevant chemical and physical processes are generally embedded within the model computer code, rendering it extremely difficult to evaluate the uncertainty that arises from any specific parameterization. For example, evaluations by Derwent et al. (2016, 2018, 2021) identify important uncertainties in CTM results, but the determination of avenues to correct the model deficiencies was not possible. However, of course, our simple observation-based model, which does not attempt to simulate the relevant processes in detail, cannot provide a detailed understanding of the chemical or physical processes that contribute to ozone formation, such as that available from CTMs. Consequently, its applications are quite limited, preventing it from performing many of the tasks for which detailed CTMs are utilized. In summary, neither CTMs nor our simpler approach alone can give the desired full understanding of the tropospheric ozone distribution – hence the need for a robust modeling hierarchy.

Continuing to guide US ozone air quality policy development requires this modeling hierarchy to address new challenges. For more than 5 decades, policies have primarily focused on urban ozone produced from precursors emitted by mobile and industrial sources; the contributions from transported background ozone and photochemical production driven by other emission sources have received much less attention. However, as we demonstrate in this and earlier papers, this original anthropogenic contribution has been so effectively reduced (a decrease of more than a factor of 6 from 1980 to 2020) that the background contribution now predominates throughout the US. Accordingly, increased attention must now be placed on a variety of additional, less well-quantified anthropogenic sources, notably including emissions from wildfires, oil and gas production, and agricultural activities. Present-day CTMs simulate ozone production from these additional sources, but the results have substantial uncertainties arising from the necessity of developing and incorporating a manifold of additional parameterizations for their treatment. Observation-based modeling can also give insights into the influences of these additional sources without the need for such parameterizations; these insights arise from temporal and spatial correlations

between observed ozone concentrations and emissions from these sources. For example, in this work, we quantify small but significant ODV contributions from wildfires in central urban areas of the southwestern US; similar analyses for urban areas of the Pacific Northwest are given by Parrish et al. (2022). In previous papers (Parrish et al., 2017, 2022), we have identified indications that soil emissions of nitrogen oxides in California's regions of intense, fertilized agricultural activity (i.e., the Imperial, San Joaquin and Salinas valleys) increase ODVs by 5–15 ppb, which has been substantiated by further empirical studies (Wang et al., 2023). We conclude that a robust understanding of the spatial and temporal distribution of US ozone concentrations requires a model hierarchy that includes both CTMs and observation-based models as well as, hopefully, other modeling approaches. We can have confidence in that understanding only when all of the models can converge to a consistent quantification of that distribution, and only then can reliable policy guidance be provided.

Data availability. The California MDA8 ozone concentrations were obtained from the California Air Resources Board archive (https://www.arb.ca.gov/adam/index.html, California Air Resources Board, 2023). The ODVs were obtained from EPA's Air Quality System (AQS) data archive (https://www.epa.gov/aqs, U.S. EPA, 2023).

Supplement. The supplement related to this article is available online at: https://doi.org/10.5194/acp-25-263-2025-supplement.

Author contributions. DDP was responsible for the overall design. ICF provided analysis. DDP wrote the paper with input from ICF and RGD. All authors edited and revised the manuscript.

Competing interests. The contact author received financial support from the Coordinating Research Council, Inc. (CRC). The CRC is a non-profit corporation supported by the petroleum and automotive equipment industries. CRC operates via committees made up of technical experts from industry and government who voluntarily participate. The four main areas of research within CRC are as follows: air pollution (atmospheric and engineering studies); aviation fuels, lubricants and equipment performance; heavy-duty vehicle fuels, lubricants and equipment performance (e.g., diesel trucks); and light-duty vehicle fuels, lubricants and equipment performance (e.g., passenger cars). CRC's function is to provide the mechanism for joint research conducted by the two industries that will help to determine the optimum combination of petroleum products and automotive equipment. CRC's work is limited to research that is mutually beneficial to the two industries involved. The contact author has declared that none of the authors has any other competing interests.

Disclaimer. Publisher's note: Copernicus Publications remains neutral with regard to jurisdictional claims made in the text, published maps, institutional affiliations, or any other geographical representation in this paper. While Copernicus Publications makes every effort to include appropriate place names, the final responsibility lies with the authors.

Acknowledgements. David D. Parrish's effort was supported by the CRC through contract no. A-129. Ian C. Faloona's effort was supported by the USDA National Institute of Food and Agriculture (Hatch project CA-D-LAW-2481-H, "Understanding Background Atmospheric Composition, Regional Emissions, and Transport Patterns Across CA"). Richard G. Derwent's efforts were pro bono.

Financial support. This research has been supported by the Coordinating Research Council, Inc. (contract no. A-129) and the US Department of Agriculture (grant no. CA-D-LAW-2481-H).

Review statement. This paper was edited by Anne Perring and reviewed by three anonymous referees.

References

Abalos, M., Orbe, C., Kinnison, D. E., Plummer, D., Oman, L. D., Jöckel, P., Morgenstern, O., Garcia, R. R., Zeng, G., Stone, K. A., and Dameris, M.: Future trends in stratosphere-to-troposphere transport in CCMI models, Atmos. Chem. Phys., 20, 6883–6901, https://doi.org/10.5194/acp-20-6883-2020, 2020.

Abeleira, A. J. and Farmer, D. K.: Summer ozone in the northern Front Range metropolitan area: weekend–weekday effects, temperature dependences, and the impact of drought, Atmos. Chem. Phys., 17, 6517–6529, https://doi.org/10.5194/acp-17-6517-2017, 2017.

Ahmadi, M. and John, K.: Statistical evaluation of the impact of shale gas activities on ozone pollution in North Texas, Sci. Total Environ., 536, 457–467, 2015.

Berlin, S. R., Langford, A. O., Estes, M., Dong, M., and Parrish, D. D.: Magnitude, decadal changes and impact of regional background ozone transported into the greater Houston, Texas area, Environ. Sci. Technol., 47, 13985–13992, https://doi.org/10.1021/es4037644, 2013.

Burke, M., Driscoll, A., Heft-Neal, S., Xue, J., Burney, J., and Wara, M.: The changing risk and burden of wildfire in the United States, P. Natl. Acad. Sci. USA, 118, e2011048118, https://doi.org/10.1073/pnas.2011048118, 2021.

California Air Resources Board: Air Quality Data Statistics, California Air Resources Board data archive, https://www.arb.ca.gov/adam/index.html, last access: 10 October 2023.

Cooper, O. R., Oltmans, S. J., Johnson, B. J., Brioude, J., Angevine, W., Trainer, M., Parrish, D. D., Ryerson, T. R., Pollack, I., Cullis, P. D., Ives, M. A., Tarasick, D. W., Al-Saadi, J., and Stajner, I.: Measurement of western U.S. baseline ozone from the surface to the tropopause and assessment of downwind impact regions, J. Geophys. Res., 116, D00V03, https://doi.org/10.1029/2011JD016095, 2011.

Cooper, O. R., Parrish, D. D., Ziemke, J., Balashov, N. V., Cupeiro, M., Galbally, I. E., Gilge, S., Horowitz, L., Jensen, N. R., Lamarque, J.-F., Naik, V., Oltmans, S. J., Schwab, J., Shindell, D. T., Thompson, A. M., Thouret, V., Wang, Y., and Zbinden, R. M.: Global distribution and trends of tropospheric ozone: An observation-based review, Elem. Sci. Anth., 2, 000029, https://doi.org/10.12952/journal.elementa.000029, 2014.

Cooper, O. R., Langford, A. O., Parrish, D. D., and Fahey, D. W.: Challenges of a lowered US ozone standard, Science, 348, 1096–1097, https://doi.org/10.1126/science.aaa5748, 2015.

Cooper, O. R., Schultz, M. G., Schröder, S., Chang, K.-L., Gaudel, A., Benítez, G. C., Cuevas, E., Fröhlich, M., Galbally, I. E., Molloy, S., Kubistin, D., Lu, X., McClure-Begley, A., Nédélec, P., O'Brien, J., Oltmans, S. J., Petropavlovskikh, I., Ries, L., Senik, I., Sjöberg, K., Solberg, S., Spain, G. T., Spangl, W., Steinbacher, M., Tarasick, D., Thouret, V., and Xu, X.: Multi-decadal surface ozone trends at globally distributed remote locations, Elem. Sci. Anth., 8, 23, https://doi.org/10.1525/elementa.420, 2020.

Derwent, R. G., Parrish, D. D., Galbally, I. E., Stevenson, D. S., Doherty, R. M., Young, P. J., and Shallcross, D. E.: Interhemispheric differences in seasonal cycles of tropospheric ozone in the marine boundary layer: Observation-model comparisons, J. Geophys. Res.-Atmos., 121, 11075–11085, https://doi.org/10.1002/2016JD024836, 2016.

Derwent, R. G., Parrish, D. D., Galbally, I. E., Stevenson, D. S., Doherty, R. M., Naik, V., and Young, P. J.: Uncertainties in models of tropospheric ozone based on Monte Carlo analysis: Tropospheric ozone burdens, atmospheric lifetimes and surface distributions, Atmos. Environ., 180, 93–102, https://doi.org/10.1016/j.atmosenv.2018.02.047, 2018.

Derwent, R. G., Parrish, D. D., Archibald, A. T., Deushi, M., Bauer, S. E., Tsigaridis, K., Shindell, D., Horowitz, L. W., Anwar, M., Khan, H., and Shallcross D. E.: Intercomparison of the representations of the atmospheric chemistry of preindustrial methane and ozone in earth system and other global chemistry-transport models, Atmos. Environ., 248, 118248, https://doi.org/10.1016/j.atmosenv.2021.118248, 2021.

Derwent, R. G., Parrish, D. D., and Faloona, I. C.: Opinion: Establishing a science-into-policy process for tropospheric ozone assessment, Atmos. Chem. Phys., 23, 13613–13623, https://doi.org/10.5194/acp-23-13613-2023, 2023.

Dolwick, P., Akhtar, F., Baker, K. R., Possiel, N., Simon, H., and Tonnesen, G.: Comparison of background ozone estimates over the western United States based on two separate model methodologies, Atmos. Environ., 109, 282–296, https://doi.org/10.1016/j.atmosenv.2015.01.005, 2015.

Emanuel, K.: The Relevance of Theory for Contemporary Research in Atmospheres, Oceans, and Climate, AGU Advances, 1, e2019AV000129, https://doi.org/10.1029/2019AV000129, 2020.

Evans, J. M. and Helmig, D.: Investigation of the influence of transport from oil and natural gas regions on elevated ozone levels in the northern Colorado front range, J. Air Waste Manage., 67, 196–211, https://doi.org/10.1080/10962247.2016.1226989, 2017.

Faloona, I. C., Chiao, S., Eiserloh, A. J., Alvarez II, R. J., Kirgis, G., Langford, A. O., Senff, C. J., Caputi, D., Hu, A., Iraci, L. T., Yates E. L., Marrero, J. E., Ryoo, J.-M., Conley, S., Tanrikulu, S., Xu, J., and Kuwayama, T.: The California baseline ozone transport study (CABOTS), B. Am. Meteorol. Soc., 101, E427–E445, https://doi.org/10.1175/BAMS-D-18-0302.1, 2020.

Faloona, I. C., Wang, Y., Derwent, R. G., and Parrish, D. D.: Maximum Ozone Concentrations in Inland California: Contributions from Background Ozone, Urban Ozone Transport, Agriculture and Wildfires, in preparation, 2025.

Fiore, A. M., Oberman, J. T., Lin, M. Y., Zhang, L., Clifton, O. E., Jacob, D. J., Naik, V., Horowitz, L. W., Pinto, J. P., and Milly, G. P.:Estimating North American background ozone in U.S. surface air with two independent global models: Variability, uncertainties, and recommendations, Atmos. Environ., 96, 284–300, https://doi.org/10.1016/j.atmosenv.2014.07.045, 2014.

Flynn, M. T., Mattson, E. J., Jaffe, D. A., and Gratz, L. E.: Spatial patterns in summertime surface ozone in the Southern Front Range of the U.S. Rocky Mountains, Elem. Sci. Anth., 9, 1, https://doi.org/10.1525/elementa.2020.00104, 2021.

Geddes, J. A., Pusede, S. E., and Wong, A. Y. H.: Changes in the relative importance of biogenic isoprene and soil NO_x emissions on ozone concentrations in nonattainment areas of the United States, J. Geophys. Res.-Atmos., 127, e2021JD036361, https://doi.org/10.1029/2021JD036361, 2022.

Gkatzelis, G. I., Gilman, J. B., Brown, S. S., Eskes, H., Gomes, A. R., Lange, A. C., and Kiendler-Scharr, A.: The global impacts of COVID-19 lockdowns on urban air pollution: A critical review and recommendations, Elem. Sci. Anth., 9, 00176, https://doi.org/10.1525/elementa.2021.00176, 2021.

Gong, X., Kaulfus, A., Nair, U., and Jaffe, D. A.: Quantifying O_3 impacts in urban areas due to wildfires using a generalized additive model, Environ. Sci. Technol., 51, 22, 13216–13223, https://doi.org/10.1021/acs.est.7b03130, 2017.

Held, I. M.: The gap between simulation and understanding in climate modeling, B. Am. Meteorol. Soc., 86, 1609–1614, https://doi.org/10.1175/Bams-86-11-1609, 2005.

Hogrefe, C., Liu, P., Pouliot, G., Mathur, R., Roselle, S., Flemming, J., Lin, M., and Park, R. J.: Impacts of different characterizations of large-scale background on simulated regional-scale ozone over the continental United States, Atmos. Chem. Phys., 18, 3839–3864, https://doi.org/10.5194/acp-18-3839-2018, 2018.

Hosseinpour, F., Kumar, N., Tran, T., and Knipping, E.: Using machine learning to improve the estimate of U.S. background ozone, Atmos. Environ., 316, 120145, https://doi.org/10.1016/j.atmosenv.2023.120145, 2024.

Hu, L., Jacob, D. J., Liu, X., Zhang, Y., Zhang, L., Kim, P. S., Sulprizio, M. P., and Yantosca R. M.: Global budget of tropospheric ozone: Evaluating recent model advances with satellite (OMI), aircraft (IAGOS), and ozonesonde observations, Atmos. Environ., 167, 323–334, 2017.

Iglesias, V., Balch, J. K., and Travis, W. R.: U.S. fires became larger, more frequent, and more widespread in the 2000s, Sci. Adv., 8, eabc0020, https://doi.org/10.1126/sciadv.abc0020, 2022.

Jaffe, D., Price, H., Parrish, D. D., Goldstein, A., and Harris, J.: Increasing background ozone during spring on the west coast of North America, Geophys. Res. Lett., 30, 1613, https://doi.org/10.1029/2003GL017024, 2003.

Jaffe, D. A. and Ray, J.: Increase in Ozone at Rural Sites in the Western U.S., Atmos. Environ., 41, 5452–5463, 2007.

Jaffe, D. A., Cooper, O. R., Fiore, A. M., Henderson, B. H., Tonneson, G. S., Russell, A. G., Henze, D. K., Langford, A. O., Lin, M., and Moore, T.: Scientific assessment of background ozone

over the U.S.: Implications for air quality management, Elem. Sci. Anth., 6, 56, https://doi.org/10.1525/elementa.309, 2018.

Karle, N. N., Fitzgerald, R. M., Sakai, R. K., Sullivan, D. W., and Stockwell, W. R.: Multi-Scale Atmospheric Emissions, Circulation and Meteorological Drivers of Ozone Episodes in El Paso-Juarez Airshed, Atmosphere, 12, 1575, https://doi.org/10.3390/atmos12121575, 2021.

Kim, S.-W., McDonald, B. C., Seo, S., Kim, K.-M., and Trainer, M.: Understanding the paths of surface ozone abatement in the Los Angeles Basin, J. Geophys. Res.-Atmos., 127, e2021JD035606, https://doi.org/10.1029/2021JD035606, 2022.

Langford, A. O., Alvarez II, R. J., Brioude, J., Fine, R., Gustin, M. S., Lin, M. Y., Marchbanks, R. D., Pierce, R. B., Sandberg, S. P., Senff, C. J.,Weickmann, A. M., and Williams, E. J.: Entrainment of stratospheric air and Asian pollution by the convective boundary layer in the southwestern U.S, J. Geophys. Res., 122, 1312–1337, https://doi.org/10.1002/2016JD025987, 2017.

Langford, A. O., Senff, C. J., Alvarez II, R. J., Aikin, K. C., Baidar, S., Bonin, T. A., Brewer, W. A., Brioude, J., Brown, S. S., Burley, J. D., Caputi, D. J., Conley, S. A., Cullis, P. D., Decker, Z. C. J., Evan, S., Kirgis, G., Lin, M., Pagowski, M., Peischl, J., Petropavlovskikh, I., Pierce, R. B., Ryerson, T. B., Sandberg, S. P., Sterling, C. W., Weickmann, A. M., and Zhang, L.: The *Fires, Asian, and Stratospheric Transport*–Las Vegas Ozone Study (*FAST*-LVOS), Atmos. Chem. Phys., 22, 1707–1737, https://doi.org/10.5194/acp-22-1707-2022, 2022.

Lin, M., Fiore, A. M., Horowitz, L. W., Cooper, O. R., Naik, V., Holloway, J., Johnson, B. J., Middlebrook, A. M., Oltmans, S. J., Pollack, I. B., Ryerson, T. B., Warner, J. X., Wiedinmyer, C., Wilson, J., and Wyman, B.: Transport of Asian ozone pollution into surface air over the western United States in spring, J. Geophys. Res., 117, D00V07, https://doi.org/10.1029/2011jd016961, 2012a.

Lin, M., Fiore, A. M., Cooper, O. R., Horowitz, L. W., Langford, A. O., Levy, H., Johnson, B. J., Naik, V., Oltmans, S. J., and Senff, C. J.: Springtime high surface ozone events over the western United States: Quantifying the role of stratospheric intrusions, J. Geophys. Res., 117, D00V22, https://doi.org/10.1029/2012jd018151, 2012b.

Lin, M., Horowitz, L. W., Payton, R., Fiore, A. M., and Tonnesen, G.: US surface ozone trends and extremes from 1980 to 2014: quantifying the roles of rising Asian emissions, domestic controls, wildfires, and climate, Atmos. Chem. Phys., 17, 2943–2970, https://doi.org/10.5194/acp-17-2943-2017, 2017.

Lu, Z., Streets, D. G., de Foy, B., Lamsal, L. N., Duncan, B. N., and Xing, J.: Emissions of nitrogen oxides from US urban areas: estimation from Ozone Monitoring Instrument retrievals for 2005–2014, Atmos. Chem. Phys., 15, 10367–10383, https://doi.org/10.5194/acp-15-10367-2015, 2015.

McDonald, B. C., de Gouw, J. A., Gilman, J. B., Jathar, S. H., Akherati, A., Cappa, C. D., Jimenez, J. L., Lee-Taylor, J., Hayes, P. L., McKeen, S. A., Cui, Y. Y., Kim, S.-W., Gentner, D. R., Isaacman-VanWertz, G., Goldstein, A. H., Harley, R. A., Frost, G. J., Roberts, J. M., Ryerson, T. B., and Trainer, M.: Volatile chemical products emerging as largest petrochemical source of urban organic emissions, Science, 359, 760–764, 2018.

McDuffie, E. E., Edwards, P. M., Gilman, J. B., Lerner, B. M., Dubé, W. P., Trainer, M., Wolfe, D. E., Angevine, W. M., deGouw, J.,Williams, E. J., Tevlin, A. G., Murphy, J. G., Fischer, E. V., McKeen, S., Ryerson, T. B., Peischl, J., Holloway, J. S., Aikin, K., Langford, A. O., Senff, C. J., Alvarez, R. J., Hall, S. R., Ullmann, K., Lantz, K. O., and Brown, S. S.: Influence of oil and gas emissions on summertime ozone in the Colorado Northern Front Range, J. Geophys. Res.-Atmos., 121, 8712–8729, 2016.

McKeen, S. A., Wotawa, G., Parrish, D. D., Holloway, J. S., Burh, M. P., Hübler, G., Fehsenfeld, F. C., and Meagher, J. F.: Ozone production from Canadian wildfires during June and July of 1995, J. Geophys. Res., 107, 4192, https://doi.org/10.1029/2001JD000697, 2002.

Nopmongcol, U., Alvarez, Y., Jung, J., Grant, J., Kumar, N., and Yarwood, G.: Source contributions to United States ozone and particulate matter over five decades from 1970 to 2020, Atmos. Environ., 167, 116–128, 2017.

Oltmans, S. J., Lefohn, A. S., Harris, J. M., and Shadwick, D. S.: Background ozone levels of air entering the west coast of the U.S., and assessment of longer-term changes, Atmos. Environ., 42, 6020–6038, https://doi.org/10.1016/j.atmosenv.2008.03.034, 2008.

Parrish, D. D. and Ennis, C. A.: Estimating background contributions and US anthropogenic enhancements to maximum ozone concentrations in the northern US, Atmos. Chem. Phys., 19, 12587–12605, https://doi.org/10.5194/acp-19-12587-2019, 2019.

Parrish, D. D. and Stockwell, W. R.: Urbanization and air pollution: Then and now, Eos: Earth & Space Science News, 96, 10–15, 2015.

Parrish, D. D., Millet, D. B., and Goldstein, A. H.: Increasing ozone in marine boundary layer inflow at the west coasts of North America and Europe, Atmos. Chem. Phys., 9, 1303–1323, https://doi.org/10.5194/acp-9-1303-2009, 2009.

Parrish, D. D., Aikin, K. C., Oltmans, S. J., Johnson, B. J., Ives, M., and Sweeny, C.: Impact of transported background ozone inflow on summertime air quality in a California ozone exceedance area, Atmos. Chem. Phys., 10, 10093–10109, https://doi.org/10.5194/acp-10-10093-2010, 2010.

Parrish, D. D., Law, K. S., Staehelin, J., Derwent, R., Cooper, O. R., Tanimoto, H., Volz-Thomas, A., Gilge, S., Scheel, H.-E., Steinbacher, M., and Chan, E.: Long-term changes in lower tropospheric baseline ozone concentrations at northern mid-latitudes, Atmos. Chem. Phys., 12, 11485–11504, https://doi.org/10.5194/acp-12-11485-2012, 2012.

Parrish, D. D., Xu, J,. Croes, B., and Shao, M.: Air Quality Improvement in Los Angeles - Perspectives for Developing Cities, Front. Environ. Sci. Eng., 10, 11, https://doi.org/10.1007/s11783-016-0859-5, 2016.

Parrish, D. D., Young, L. M., Newman, M. H., Aikin, K. C., and Ryerson, T. B.: Ozone design values in southern California's air basins: Temporal evolution and U.S. background contribution, J. Geophys. Res., 122, 11166–11182, 2017.

Parrish, D. D., Derwent, R. G., Steinbrecht, W., Stübi, R., VanMalderen, R., Steinbacher, M., Trickl, T., Ries, L., and Xu, X.: Zonal similarity of long-term changes and seasonal cycles of baseline ozone at northern midlatitudes, J. Geophys. Res.-Atmos., 125, e2019JD031908, https://doi.org/10.1029/2019JD031908, 2020.

Parrish, D. D., Derwent, R. G., and Faloona, I. C.: Long-term baseline ozone changes in the Western US: A syn-

thesis of analyses, J. Air Waste Manage., 71, 1397–1406, https://doi.org/10.1080/10962247.2021.1945706, 2021a.

Parrish, D. D., Derwent, R. G., and Staehelin, J.: Long-term changes in northern mid-latitude tropospheric ozone concentrations: Synthesis of two recent analyses, Atmos. Environ., 248, 118227, https://doi.org/10.1016/j.atmosenv.2021.118227, 2021b.

Parrish, D. D., Derwent, R. G., and Faloona, I. C.: Observational-based assessment of contributions to maximum ozone concentrations in the western US, J. Air Waste Manage., 72, 434–454, https://doi.org/10.1080/10962247.2022.2050962, 2022.

Schnell, R. C., Oltmans, S. J., Neely, R. R., Endres, M. S., Molenar, J. V., and White, A. B.: Rapid photochemical production of ozone at high concentrations in a rural site during winter, Nat. Geosci., 2, 120–122, 2009.

Simon, H., Reff, A., Wells, B., Xing, J., and Frank, N.: Ozone trends across the United States over a period of decreasing NO_x and VOC emissions, Environ. Sci. Technol., 49, 186–195, https://doi.org/10.1021/es504514z, 2015.

Škerlak, B., Sprenger, M., and Wernli, H.: A global climatology of stratosphere–troposphere exchange using the ERA-Interim data set from 1979 to 2011, Atmos. Chem. Phys., 14, 913–937, https://doi.org/10.5194/acp-14-913-2014, 2014.

Skipper, T. N., Hu, Y., Odman, M. T., Henderson, B. H., Hogrefe, C., Mathur, R., and Russell, A. G.: Estimating US Background Ozone Using Data Fusion, Environ. Sci. Technol., 55, 4504–4512, https://doi.org/10.1021/acs.est.0c08625, 2021.

Sprenger, M. and Wernli, H.: A northern hemisphere climatology of cross-tropopause exchange for the ERA15 time period (1979–1993), J. Geophys. Res., 108, 8521, https://doi.org/10.1029/2002JD002636, 2003.

U.S. EPA: Ambient Air Pollution Data, EPA's Air Quality System (AQS) data archive, https://www.epa.gov/aqs, last access: 9 November 2023.

Wang, Y., Faloona, I. C., and Houlton, B. Z.: Satellite NO_2 trends reveal pervasive impacts of wildfire and soil emissions across California landscapes, Environ. Res. Lett., 18, 094032, https://doi.org/10.1088/1748-9326/acec5f, 2023.

Westerling, A. L.: Increasing western US forest wildfire activity: sensitivity to changes in the timing of spring, Philos. Trans. R. Soc. Lond. B Biol. Sci., 371, 20150178, https://doi.org/10.1098/rstb.2015.0178, 2016.

Westerling, A. L., Hidalgo, H. G., Cayan, D. R., and Swetnam, T. W.: Warming and earlier spring increase western US forest wildfire activity, Science, 313, 940–943, 2006.

Yates, E. L., Iraci, L. T., Austerberry, D., Pierce, R. B., Roby, M. C., Tadić, J. M., Loewenstein, M., and Gore, W.: Characterizing the impacts of vertical transport and photochemical ozone production on an exceedance area, Atmos. Environ., 109, 342–350, 2015.

Zhang, J., Yongjie, W., and Zhangfu, F.: Ozone Pollution: A Major Health Hazard Worldwide, Front. Immunol., 10, 2518, https://doi.org/10.3389/fimmu.2019.02518, 2019.

Zhang, L., Lin, M., Langford, A. O., Horowitz, L. W., Senff, C. J., Klovenski, E., Wang, Y., Alvarez II, R. J., Petropavlovskikh, I., Cullis, P., Sterling, C. W., Peischl, J., Ryerson, T. B., Brown, S. S., Decker, Z. C. J., Kirgis, G., and Conley, S.: Characterizing sources of high surface ozone events in the southwestern US with intensive field measurements and two global models, Atmos. Chem. Phys., 20, 10379–10400, https://doi.org/10.5194/acp-20-10379-2020, 2020.

Ziemke, J. R., Chandra, S., Labow, G. J., Bhartia, P. K., Froidevaux, L., and Witte, J. C.: A global climatology of tropospheric and stratospheric ozone derived from Aura OMI and MLS measurements, Atmos. Chem. Phys., 11, 9237–9251, https://doi.org/10.5194/acp-11-9237-2011, 2011.